



Ubx5-Cdc48 assists the protease Wss1 at DNA-protein crosslink sites in yeast

Audrey Noireterre^{1*} , Nataliia Serbyn^{1,†,‡}, Ivona Bagdiul¹ & Françoise Stutz^{1,‡} 

Abstract

DNA-protein crosslinks (DPCs) pose a serious threat to genome stability. The yeast proteases Wss1, 26S proteasome, and Ddi1 are safeguards of genome integrity by acting on a plethora of DNA-bound proteins in different cellular contexts. The AAA ATPase Cdc48/p97 is known to assist Wss1/SPRTN in clearing DNA-bound complexes; however, its contribution to DPC proteolysis remains unclear. Here, we show that the Cdc48 adaptor Ubx5 is detrimental in yeast mutants defective in DPC processing. Using an inducible site-specific crosslink, we show that Ubx5 accumulates at persistent DPC lesions in the absence of Wss1, which prevents their efficient removal from the DNA. Abolishing Cdc48 binding or complete loss of Ubx5 suppresses sensitivity of *wss1Δ* cells to DPC-inducing agents by favoring alternate repair pathways. We provide evidence for cooperation of Ubx5-Cdc48 and Wss1 in the genotoxin-induced degradation of RNA polymerase II (RNAPII), a described candidate substrate of Wss1. We propose that Ubx5-Cdc48 assists Wss1 for proteolysis of a subset of DNA-bound proteins. Together, our findings reveal a central role for Ubx5 in DPC clearance and repair.

Keywords Cdc48/p97; DNA-protein crosslink; protease; UBX protein; yeast

Subject Categories DNA Replication, Recombination & Repair; Post-translational Modifications & Proteolysis

DOI 10.15252/emboj.2023113609 | Received 25 January 2023 | Revised 14 April 2023 | Accepted 24 April 2023 | Published online 5 May 2023

The EMBO Journal (2023) 42: e113609

Introduction

DNA-protein crosslinks (DPCs), also known as protein-DNA adducts, are formed by the covalent association of a protein with DNA. If left unresolved, these highly mutagenic and cytotoxic lesions can interfere with essential DNA transactions, cause a severe block to the progression of replication and transcription machinery, and therefore jeopardize the fidelity of genome integrity (Stinglele *et al.*, 2017). DPCs are classified into two groups, non-enzymatic and enzymatic, depending on the nature of the crosslinked protein and

the triggering mechanism that leads to DPC formation. Non-enzymatic DPCs arise from non-specific crosslinking after exposure to metabolic products such as formaldehyde or acetaldehyde or by the action of exogenous agents (UV-light, IR, etc.), while enzymatic DPCs are the result of abortive enzymatic reactions that require the establishment of a covalent DNA-enzyme reaction intermediate (Stinglele *et al.*, 2015; Stinglele & Jentsch, 2015; Vaz *et al.*, 2017; Zhang *et al.*, 2020).

DNA Topoisomerase 1 (Top1) is prone to enzymatic DPC formation, as it forms a covalent link with DNA to relax torsional stress that emerges during DNA replication and transcription (Pommier *et al.*, 2016). To do so, Top1 nicks DNA and covalently binds one strand to assemble in a transient entity known as a Top1 cleavage complex (Top1cc; Pommier, 2006). Top1-DNA crosslinks can appear when the enzymatic cleavage occurs close to certain DNA lesions (abasic sites, DNA breaks, base mismatch, etc.) or be induced by camptothecin (CPT), a Top1-poison that inserts into the catalytic pocket of Top1 and stabilizes Top1ccs (Staker *et al.*, 2002). Using a similar catalytic mechanism, F1p recombinase introduces a nick at a specific *FRT* target site. A F1p mutant carrying the point mutation H305L will drive the formation of a stable covalent crosslink upon *FRT* cleavage. The genetic requirements for cells to repair this DPC-like lesion on DNA are the same as for cells treated with the Top1 poison CPT (Nielsen *et al.*, 2009; Serbyn *et al.*, 2020, 2021).

Along with the canonical DSB repair pathways such as nucleotide excision repair (NER) and homologous recombination (HR; Ide *et al.*, 2011), numerous other pathways have been implicated in the processing of trapped-Top1ccs (Pommier *et al.*, 2014; Vaz *et al.*, 2017; Fielden *et al.*, 2018; Ide *et al.*, 2018). In yeast, the tyrosyl-DNA phosphodiesterase Tdp1, which directly hydrolyzes the bond between Top1 and the DNA, was among the first DNA repair enzymes described to have relevance for the elimination of Top1-DNA crosslinks (Yang *et al.*, 1996; Pouliot *et al.*, 1999, 2001). Tdp1 is not able to process intact Top1ccs and prior proteolytic digestion or denaturation is essential to enable hydrolysis by Tdp1 (Yang *et al.*, 1996; Debethune *et al.*, 2002; Pommier *et al.*, 2014). Recently, the yeast proteases Wss1 (SPRTN or DVC1 in mammals), Ddi1, and 26S proteasome were shown to participate in the proteolysis of the protein moiety of a DPC (Stinglele *et al.*, 2014; Serbyn *et al.*, 2020). It is proposed that remodeling or initial processing of the adducts is

¹ Department of Molecular and Cellular Biology, University of Geneva, Geneva, Switzerland

*Corresponding author. Tel: +41223796741; E-mail: audrey.noireterre@unige.ch

**Corresponding author. Tel: +41223796729; E-mail: francoise.stutz@unige.ch

[†]Present address: Department of Pediatric Oncology, Dana-Farber Cancer Institute, Boston, MA, USA

[‡]Present address: Department of Cellular Biology, Blavatnik Institute, Harvard Medical School, Boston, MA, USA

required before proteolysis, which may involve the AAA ATPase Cdc48 (known as p97/VCP; Nie *et al.*, 2012; Stingle *et al.*, 2014; Balakirev *et al.*, 2015; Fielden *et al.*, 2020).

Cdc48/p97 is an abundant essential chaperone involved in a wide variety of cellular processes, including but not limited to cell cycle regulation, membrane fusion, transcriptional control, and ubiquitin-dependent protein degradation (Woodman, 2003; Ye, 2006; White & Lauring, 2007; Stach & Freemont, 2017). Several studies investigated its role in DNA replication (Yamada *et al.*, 2000; Mouysset *et al.*, 2008; Deichsel *et al.*, 2009; Ramadan *et al.*, 2017) and DNA repair (Zhang *et al.*, 2000; Vaz *et al.*, 2013; Torrecilla *et al.*, 2017), including DPC repair. In most of the processes, Cdc48/p97 processing is initiated by unfolding of ubiquitin conjugated to its targets (Ye, 2006; Twomey *et al.*, 2019). The substrate specificity is achieved through interaction with numerous regulatory adaptors (Hanzelmann & Schindelin, 2017), of which UBX proteins constitute the largest known group (Schuberth & Buchberger, 2008). Supporting the idea of a role for Cdc48/p97 in DNA-bound protein clearance, Cdc48/p97 mediates chromatin extraction and disassembly of some protein complexes (Jentsch & Rumpf, 2007; Shcherbik & Haines, 2007; Maric *et al.*, 2014; Frattini *et al.*, 2017; Ramadan *et al.*, 2017). It was linked to processes involved in SPRTN/Wss1 proteolysis (Lin *et al.*, 2008; Davis *et al.*, 2012; Ghosal *et al.*, 2012; Mosbech *et al.*, 2012; Nie *et al.*, 2012; Stingle *et al.*, 2014; Balakirev *et al.*, 2015; Maskey *et al.*, 2017; Fielden *et al.*, 2020; Kroning *et al.*, 2022) and is also required for proteasome-mediated degradation of stalled RNA Polymerase II (RNAPII) following UV-induced DNA damage (Verma *et al.*, 2011; Lafon *et al.*, 2015; He *et al.*, 2017). Particularly, a specialized complex containing mammalian p97 and its cofactor TEX264 is required for clearance of TOP1-DNA adducts by SPRTN (Fielden *et al.*, 2020), raising the question of cofactor specificity regarding DPC substrates. The ability of Cdc48/p97 to counteract DPCs appears crucial; however, the mechanistic basis of how it is achieved is still not fully defined.

In this work, we investigate the involvement in DPC repair of Ubx5, a Cdc48 co-factor of the UBX protein family that has previously been implicated in UV-induced degradation of the largest subunit of RNAPII, Rpb1 (Verma *et al.*, 2011). Based on our findings, Ubx5 has a negative effect in *Saccharomyces cerevisiae* mutant strains exhibiting DPC persistence related to the unavailability of the DPC-protease Wss1. By using an *in vivo* inducible DPC system, we observed that Ubx5 and Cdc48 accumulation at sites of unrepaired DPC lesions delays their clearance. We further demonstrate that loss of interaction between Ubx5 and Cdc48 is sufficient to suppress the growth phenotype and drug sensitivity of yeast mutant strains accumulating DPCs. Finally, loss of Ubx5 restores the impaired genotoxin-induced degradation of Rpb1 in the absence of the protease Wss1, in a Ddi1-dependent manner. We propose a new mechanism in which Ubx5 mediates Cdc48 recruitment to adducts on chromatin, such as DNA-protein crosslinks or stalled RNA Polymerase II.

Results

Multiple Cdc48 co-factors suppress effects of mutations affecting Top1-DNA crosslinks

Aiming to unravel Cdc48 adaptors that define substrate-specificity in DPC repair, we intersected the list of known CDC48 interactors

with the genetic network of the *tdp1-degron* + *auxin wss1Δ* (*tdp1wss1*) mutant defective in Top1cc repair. A list of physical and genetic CDC48 interactors was extracted from the yeast Saccharomyces Genome Database (SGD; Cherry *et al.*, 1997; Fig EV1A). For these selected genes, we then analyzed the relative number of transposition events in auxin-treated *tdp1-degron wss1Δ* mutant (Serbyn *et al.*, 2020; Fig 1A). We noted increased transpositions in the UBX5 gene body (Fig 1B) and confirmed that *ubx5Δ* substantially rescues the growth phenotype of freshly dissected yeast spores (Figs 1C and EV1B), as well as the CPT sensitivity (Fig 1D) of the *tdp1wss1* double mutant defective in Top1ccs repair (Stingle *et al.*, 2014; Balakirev *et al.*, 2015). It is worth pointing out that Ufd1 and Npl4, both known to be core adaptors of the Cdc48-Ufd1-Npl4 complex recruited to double-strand breaks (DSBs; Meerang *et al.*, 2011) and DNA-bound proteins (Balakirev *et al.*, 2015), are suppressors of *tdp1wss1* as well (Fig 1A). Moreover, Ubx5 protein levels are decreased in the *tdp1-degron wss1Δ* mutant, emphasizing the negative effect of Ubx5 in that cellular context (Fig 1E and F; *tdp1-degron wss1Δ* + auxin). Loss of Wss1 alone already causes reduction of steady-state Ubx5 levels (Fig 1E and F; *tdp1-degron wss1Δ* no auxin), suggesting that the *ubx5Δ* suppression may represent the adaptive response to Wss1 deficiency. From these data, we presumed that Ubx5 may have an inhibitory effect in the absence of the repair enzymes Wss1 and Tdp1.

Ubx5-Cdc48 interaction interferes with the resistance to DPCs in the absence of the Wss1 protease

Wss1 protease is required for cellular resistance against formaldehyde (FA) and hydroxyurea (HU; Fig 2A, O'Neill *et al.*, 2004; Maddi *et al.*, 2020; Serbyn *et al.*, 2020). While it is well documented that HU induces replication stress, several studies reported that HU creates free nitroxide radicals (Yarbro, 1992; King, 2003), which are prone to create DPCs (Dizdaroglu *et al.*, 1989; Nakano *et al.*, 2003), raising the possibility that DPCs may increase in response to HU. As levels of Ubx5 are downregulated in the absence of Wss1 (Fig 1E and F), we hypothesized that Ubx5 loss could restore *wss1Δ* tolerance to these DPC-inducing agents. Indeed, *ubx5Δ* reverts FA and HU hypersensitivity of the *wss1Δ* mutant to WT-like levels (Fig 2A). In contrast, *ubx5Δ* did not suppress hypersensitivity to Top1ccs in the absence of Tdp1 (Fig EV2A). From these data, we inferred that Ubx5 is genetically linked to Wss1 but not to the Top1-specific repair factor Tdp1. Given its genetic interactions, Ubx5 protein might target a broad range of DPCs for repair, similar to Wss1.

To gain further insights into Ubx5 function in DPC repair, we addressed the role of Ubx5 domains. Yeast Ubx5 consists of four known domains: an amino (N)-terminal UBA, central UAS, UIM, and a carboxyl (C)-terminal UBX (Fig 2B). To assess their role, we complemented *ubx5Δ wss1Δ* with HA-tagged Ubx5 constructs overexpressed from a galactose-inducible promoter (Fig 2C and D). Complementation by *ubx5^{ubaΔ}*, *ubx5^{uasΔ}*, or *ubx5^{uimΔ}* domain mutants was detrimental to cell growth and compromised resistance to several drugs, similar to complementation by the full-length protein (Fig 2C). However, the *ubx5^{uasΔ}* construct was not well expressed (Fig 2D), not allowing us to conclude about the role of the UAS domain. WT-like phenotypes of *ubx5^{ubaΔ}* and *ubx5^{uimΔ}* variants suggest that these domains are not involved in Wss1-related functions of Ubx5 in DNA repair. On one hand, these data argue that Wss1-linked function of Ubx5 neither

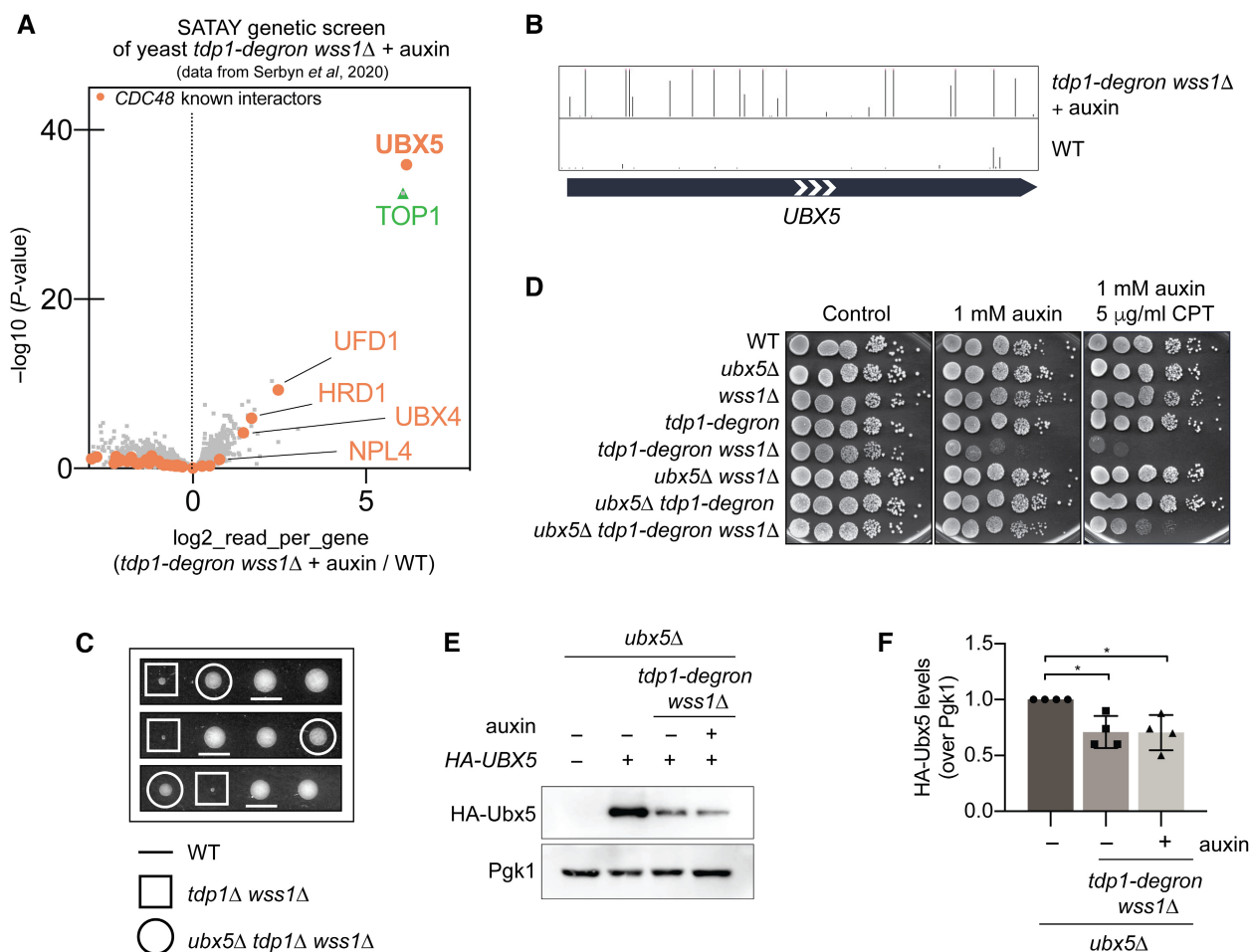


Figure 1. Cdc48 cofactor Ubx5 is a new suppressor of *tdp1Δ wss1Δ*.

A CDC48 known interactors (orange) identified as suppressors or sensitizers in the *tdp1-deg wss1Δ* SATAY transposon screen described in (Serbyn et al, 2020). The volcano plot compares the sequencing reads in *tdp1-deg wss1Δ* + auxin (*tdp1 wss1Δ*) and a pool of six unrelated SATAY libraries. Fold-change of reads per gene (\log_2 , x-axis) and corresponding P -values ($-\log_{10}$, y-axis) are plotted. The gene names of the strongest suppressors are labeled in orange. Top1 (positive control) appears in green.

B Snapshot depicting transposon coverage of *UBX5* gene body in the *tdp1-deg wss1Δ* + auxin and one of the WT libraries. The height of the bars represents the number of reads for each transposon.

C Loss of *UBX5* suppresses growth defects of *tdp1Δ wss1Δ*. Tetrads were analyzed after dissection of the diploid (*TDP1/tdp1Δ; WSS1/wss1Δ; UBX5/ubx5Δ*).

D Transposon screen validation of *UBX5*. *ubx5Δ* restores the growth of *tdp1 wss1Δ*. Cells were grown in YEPD and spotted on a medium supplemented with 1 mM auxin (for *tdp1-deg* degradation) and 5 μg/ml Camptothecin (CPT). Plates were incubated for 2 days at 30°C.

E, F Ubx5 levels are decreased in *tdp1 wss1Δ*. (E) HA-Ubx5 protein levels at steady state are compared by immunoblotting in different mutants. Mutant strains carrying the additional *ubx5Δ* mutation were complemented with a plasmid expressing HA-tagged Ubx5 from the endogenous *pUBX5* promoter. 1 mM auxin was added where indicated for 6 h to degrade *tdp1-deg*, when present. Pgk1 was used as a loading control. For quantification (F), the anti-HA signal was compared to Pgk1 and normalized to WT. Quantification of four biological replicates is presented as means ± SDs. Significance was defined by ordinary one-way ANOVA using Dunnett's multiple comparison test with WT as a control (* $P < 0.05$).

requires ubiquitin binding by the UBA domain (Husnjak & Dikic, 2012), nor interaction with ubiquitin via the UIM motif that is important for RNAPII turnover after UV treatment (den Besten et al, 2012). On the other hand, the residual ubiquitin binding of *ubx5^{ubaΔ}* and *ubx5^{uimΔ}* variants may be sufficient to cause drug sensitivity in *wss1Δ*. In the same line, the non-physiological overexpression of these constructs can potentially mask a partial loss of function.

The UBX domain of Ubx5 mediates the interaction with Cdc48 (Decottignies et al, 2004; Hartmann-Petersen et al, 2004; Schubert et al, 2004; Alexandru et al, 2008; Sasagawa et al, 2010), and we

additionally tested whether this domain is critical for DPC resistance. Interestingly, the *ubx5^{ubxΔ}* mutant was expressed at WT-like levels (Fig 2D) and showed partial rescue of *ubx5Δ wss1Δ*, even in the presence of DPC-inducing drugs (Fig 2C), suggesting the important role of Ubx5-Cdc48 interaction.

On top of that, when the genomic copy of *UBX5* was replaced by *ubx5^{ubxΔ}*, the mutant suppressed the growth defects of *tdp1Δ wss1Δ* spores (Fig EV2B), restored HU and FA resistance of *wss1Δ* (Fig EV2C and D), and restored CPT resistance of *tdp1 wss1Δ* (Fig EV2D), similarly to *ubx5Δ*.

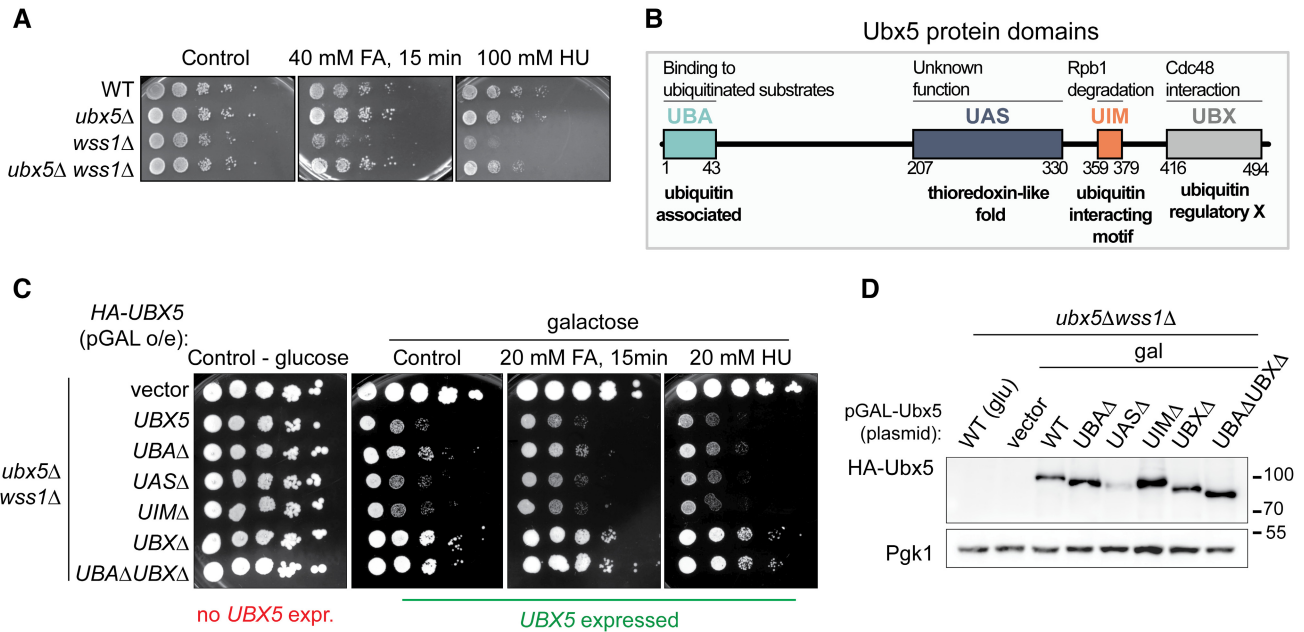


Figure 2. Loss of interaction between Cdc48 and Ubx5 restores growth of cells accumulating chromatin lesions.

- A Ubx5 loss rescues *wss1Δ* sensitivity to formaldehyde (FA) and hydroxyurea (HU). Cells were grown in YEPD and either treated with 40 mM FA for 15 min or spotted directly on 100 mM HU. Plates were incubated for 2 days at 30°C.
- B Schematic representation of Ubx5 domains. UBA domain targets Ubx5 to ubiquitinated substrates. UBX domain is a Cdc48 binding module. UIM is implicated in Rpb1 degradation after UV treatment. UAS domain has an unknown function.
- C The *UBXΔ* mutant of Ubx5 is sufficient to suppress FA and HU sensitivities of *wss1Δ*. *ubx5Δ wss1Δ* mutants were complemented with plasmids encoding HA-Ubx5-WT or HA-Ubx5 mutants overexpressed from the *pGAL* promoter; cells were grown in SC-trp and either treated with 40 mM FA for 15 min or spotted directly on 20 mM HU. Plates were prepared either with glucose (no HA-Ubx5 expression) or galactose (HA-Ubx5 expression) as the source of sugar. Plates were incubated for 2.5 days at 30°C. o/e, overexpression.
- D Protein levels of overexpressed HA-Ubx5 mutants shown in (C) were analyzed by immunoblotting (as in Fig 1E).

Altogether, these observations reinforce the idea that the Ubx5-Cdc48 interaction, mediated by the UBX domain, is severely deleterious in the absence of Wss1 upon DPC induction.

UBX proteins Ubx4 and Ubx5 are detrimental to DPC resistance

Ubx4 is another UBX-containing protein (Schuberth & Buchberger, 2008) identified as a mild suppressor of *tdp1wss1* (Fig 1A) that presents a highly transposed UBX domain in the screen (Fig EV3A). The *ubx4^{ubxΔ}* mutant partially rescued HU sensitivity of *wss1Δ* cells (Fig EV3B), while the full *UBX4* deletion did not (Fig EV3C). Similarly, *ubx4^{ubxΔ}* moderately rescued the growth defect of *tdp1wss1* (Fig EV3B), suggesting that Ubx4 could function as an alternative Cdc48 adaptor needed for DPC repair but is still required for other cellular functions. These data involve several members of the UBX proteins family in DPC repair.

We speculated that Ubx5 and Ubx4 target Cdc48 to assist Wss1 in DPC removal, each to a different extent. To explore this idea, we stressed a double *ubx4Δ ubx5Δ* mutant with several DPC inducers, as this should lead to similar sensitivities as a *WSS1* deletion (Fig EV3C and D). However and surprisingly, neither the double mutant nor the single mutants showed sensitivities to the drugs tested, also in combination with *tdp1Δ* (Fig EV3D). Despite the noxious effects of UBX proteins in the absence of Wss1, UBX proteins are not participating in all Wss1 cellular functions.

Taken together, these findings strongly suggest that the UBX proteins Ubx5 and Ubx4, both cofactors of Cdc48, are detrimental upon DPC accumulation in *wss1Δ* due to their interaction with the segregase Cdc48 via their UBX domain.

Loss of the Cdc48 adaptor Ubx5 improves repair efficiency of the crosslinked Flp

Ubx5 mutants restore a WT-like phenotype in the absence of the repair enzymes Wss1 and Tdp1. Accumulation of Top1 crosslinked to DNA in *tdp1Δ wss1Δ* was previously demonstrated (Stingele et al, 2014). We reasoned that loss of *UBX5* would lead to a decreased number of crosslinked proteins detected on DNA. To test this hypothesis, we used the previously described Flp-nick system (Fig 3A; Nielsen et al, 2009), which creates a Top1-like crosslink at a single *FRT* locus artificially introduced into chromosome VI of the yeast (*S. cerevisiae*) genome. This system uses a galactose-inducible mutant Flp recombinase *flp-H305L*, which triggers a covalent crosslink “Flp-cc” at the *FRT* site, thus allowing to precisely follow the molecular events linked to the appearance, detection, and repair of the Flp-cc. Similar to the genetic interactions observed in the *W303* strain background (Fig 1D), *ubx5Δ* also suppressed cell growth defects resulting from *flp-H305L* expression on 2% galactose in the Flp-nick system (Fig 3B). Of note, as the Flp-nick system mimics a Top1cc, endogenous Top1 was removed in the following experiments.

To monitor changes in *flp-H305L* retention at the *FRT* site, cells were first synchronized in the G1-phase of the cell cycle by the addition of α -factor prior to and during the 2 h galactose induction of the *flp-H305L* mutant (Fig 3D, upper panel). *flp-H305L* induction was then stopped with glucose and cells were released from α -factor G1 arrest and allowed to enter the cell cycle (Fig 3D, glu 60 min and 120 min; Fig 3C for cell-cycle analysis). Consistently, and as we formerly reported (Serbyn et al, 2020, 2021), *flp-H305L* was more persistent at the *FRT* site at 120 min in *tdp1 Δ wss1 Δ top1 Δ* compared to a WT strain, which showed rapid removal of the Flp-cc from the *FRT* site (Fig 3D, compare strains 1 and 2). Since *UBX5* deletion suppresses the *tdp1 Δ wss1 Δ top1 Δ* phenotype, we hypothesized that Ubx5 removal may lead to faster clearance of the protein crosslink. Indeed, Flp-cc repair dynamics in *ubx5 Δ tdp1 Δ wss1 Δ top1 Δ* was very similar to WT (Fig 3D, strain 3). These results suggest that the rescue observed in *ubx5 Δ* is probably due to a reduced amount of DPCs on the DNA.

We then reasoned that the possible negative effect of Ubx5 could be due to its presence at the damage site. We therefore tested Ubx5 recruitment at the *FRT* site using the Flp-nick system. We observed that while Ubx5 was not recruited at the Flp-cc site in a WT-like strain, there was a significant enrichment of Ubx5 upon removal of the Wss1 and Tdp1 repair enzymes that were not detected in the absence of *FRT* (Fig 3E). Notably, this great accumulation of Ubx5 at a DPC locus became significantly detectable during the S- and G2-phases, underlining the role Ubx5 may have only at certain stages of the cell cycle. A straightforward interpretation of these findings is that Ubx5 prevents the elimination of the Flp-cc (and probably Top1cc, and other DPCs) from the DNA by hyper-accumulating at the damage location when Wss1 and Tdp1 are unavailable.

Ubx5 participates in Cdc48 targeting at the crosslinked Flp

The collected data led us to wonder whether Ubx5 was involved in targeting Cdc48 to DPC sites. Indeed, we observed that Ubx5 was greatly enriched at the *FRT* site and that Ubx5 was detrimental due to its connection with Cdc48. We therefore attempted to detect Cdc48 at the crosslinked *Flp*. Although no significant enrichment was observed in a WT strain following DPC induction with galactose (Fig 4A, strain 1), Cdc48 was excessively present at the induced DPC site in the absence of Wss1 and Tdp1 (Fig 4A, strain 2). Remarkably, in line with the above-mentioned hypothesis, the Cdc48 enrichment at the *FRT* was alleviated upon loss of Ubx5 (Fig 4A, strain 3).

Regulation and targeting of Cdc48 to its multiple cellular substrates is predominantly ubiquitin-dependent (Ye, 2006). Using again the Flp-nick system, we tested whether ubiquitin occupancy at the *FRT* was changing in the different mutants examined (Fig 4B). In conjunction with what we observed before, increased ubiquitin signal was detected upon DPC induction especially in the absence of Wss1 and Tdp1 (Serbyn et al, 2021; Fig 4B). This is not surprising given that the Flp-cc remains bound at the *FRT* site in this strain background (Fig 3D, strain 2). Curiously, in the absence of Ubx5, we still detected significant accumulation of ubiquitin in the vicinity of the Flp-bound locus upon Flp-cc induction, with the highest peak after 30 min of glucose repression (Fig 4B). Later timepoints revealed that the ubiquitin kept accumulating in *tdp1 Δ wss1 Δ top1 Δ* , while it was not the case for *ubx5 Δ tdp1 Δ wss1 Δ top1 Δ* ,

respectively, correlating with the kinetics of Flp-cc remaining bound or being removed (Fig 3D). These data suggest that Cdc48 accumulates on unrepaired Flp-cc, probably targeted by Ubx5. The remaining ubiquitin species in *ubx5 Δ tdp1 Δ wss1 Δ* likely facilitate DPC repair.

Other repair pathways are active in *ubx5 Δ tdp1 Δ wss1 Δ*

We postulated that *UBX5* deletion could lead the cells toward an alternative repair pathway. The aspartic protease Ddi1 has recently been characterized as a novel DPC repair player acting in parallel to Wss1 (Svoboda et al, 2019; Serbyn et al, 2020), and it was recently shown to be a ubiquitin-dependent protease (Yip et al, 2020). We thus speculated that Ddi1 could play a role in improving the growth of *ubx5 Δ tdp1 Δ wss1 Δ* or *ubx5 Δ wss1 Δ* . By performing genetic analyses, we observed that Ddi1 was indeed essential for *ubx5 Δ tdp1 Δ wss1 Δ* survival, as spores additionally lacking Ddi1 were unable to proliferate (Figs 5A and EV4A). Likewise, Ddi1 was crucial for the viability of the *ubx5 Δ wss1 Δ* mutant under FA or HU stress (Fig 5B). Indeed, *wss1 Δ ddi1 Δ* is very sensitive to DPCs and *ubx5 Δ* is no longer proficient in suppressing *wss1 Δ* in the absence of Ddi1 (Fig 5B; Serbyn et al, 2020). However, the *ubx5 Δ ddi1 Δ* double mutant did not reveal a strong phenotype on the tested drugs (Fig 5B).

We further tested the requirements of other known Top1ccs and DPC repair factors (Liu et al, 2002; Deng et al, 2005; Pommier, 2006; Alvaro et al, 2007; Stingle et al, 2014; Sun et al, 2020b; Figs EV4B–G and EV5). Among the pathways tested, deletion of *RAD52* (homologous recombination, Fig EV4B), *RAD9* (checkpoint activation, Fig EV4C), *SGS1* (RecQ helicase, Fig EV4D), *SRS2* (anti-recombinase, Fig EV4E), *RAD27* and *MRE11* (structural nucleases, Fig EV4F and G), strongly affected growth of *ubx5 Δ tdp1 Δ wss1 Δ* spores, emphasizing the essentiality of these enzymes and their respective repair pathways to counteract DPC appearance in yeast mutants lacking Wss1 and Tdp1. Surprisingly, abrogation of the non-homologous end-joining (NHEJ) pathway (*yku70 Δ* , Fig EV5A), the translesion synthesis pathway (*rev3 Δ* , Fig EV5B) as well as deletion of the nucleotide excision repair (NER) pathway (*rad4 Δ* , Fig EV5C) had no effect on *ubx5 Δ tdp1 Δ wss1 Δ* spore survival. Taken together, these genetic analyses (Fig EV5D) show that checkpoint pathways, recombination, multiple nucleases, and Ddi1 protease facilitate the growth of *ubx5 Δ tdp1 Δ wss1 Δ* .

Ddi1 provides resistance toward DPCs to cells lacking Ubx5 and Wss1

Because the Ddi1 and Wss1 proteases work in parallel pathways, Ddi1 becomes more important when Wss1 is absent. Thus, Ddi1 expression is elevated in cells lacking Wss1 (Fig 5C and D). Interestingly, Ddi1 protein levels remained overexpressed following deletion of *UBX5* on top of the *wss1 Δ* mutation, indicating that it still plays a relevant role to help both the *ubx5 Δ wss1 Δ* and the *ubx5 Δ tdp1 Δ wss1 Δ* mutants in dealing with different sources of stress (Figs 1D, 2A, and 5B). Accordingly, ChIP-qPCR analyses at the *FRT* locus revealed that Ddi1 is recruited in *tdp1 Δ wss1 Δ top1 Δ* (Fig 5E), as previously observed (Serbyn et al, 2021). Even though the *ubx5 Δ tdp1 Δ wss1 Δ top1 Δ* mutant demonstrated more efficient Flp-cc elimination from the *FRT* (Fig 3D), Ddi1 was recruited to the same extent. This enrichment of Ddi1 suggests that it is a key contributor

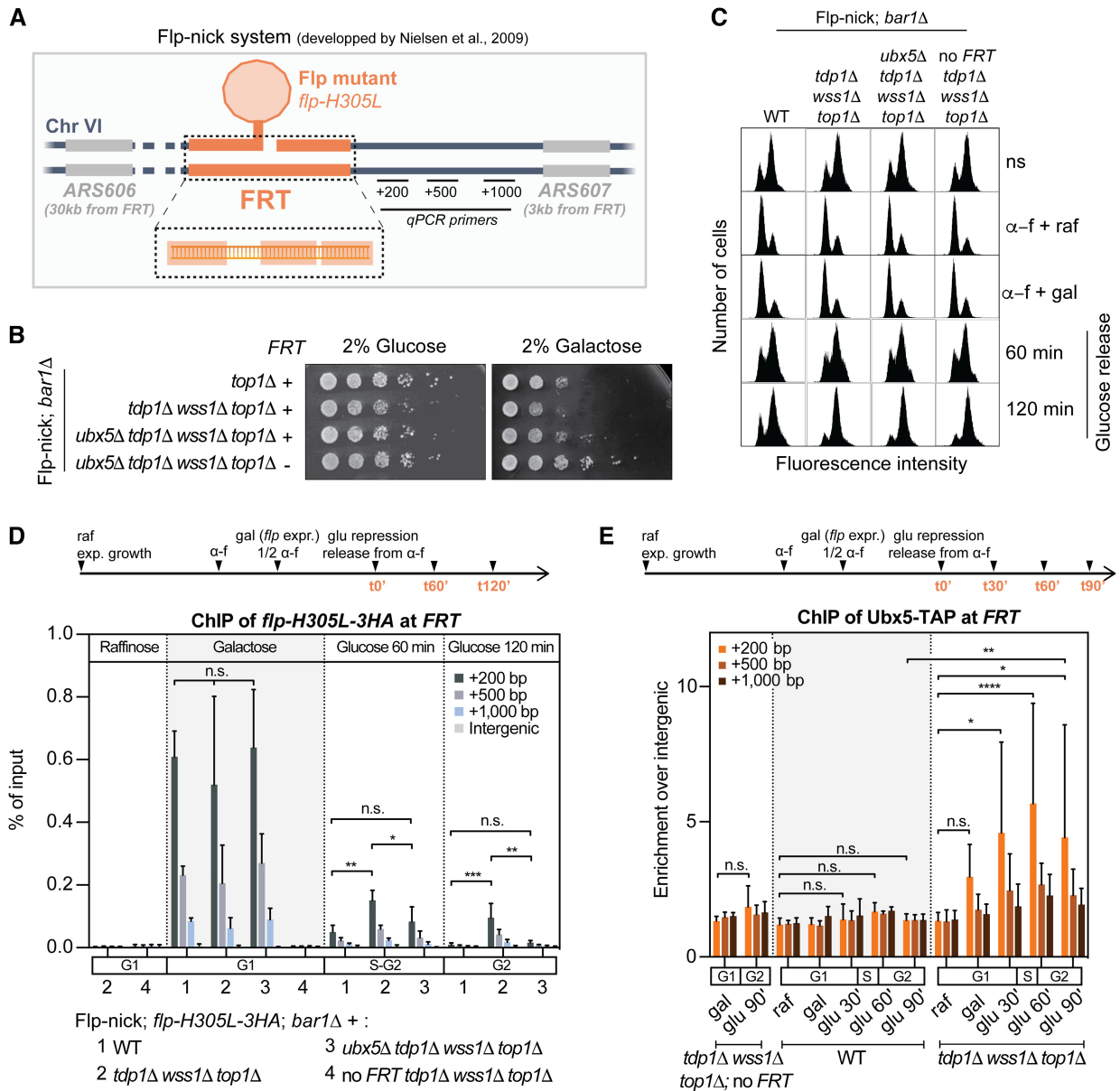


Figure 3. Loss of Ubx5 has a suppressing effect on crosslinked Flp.

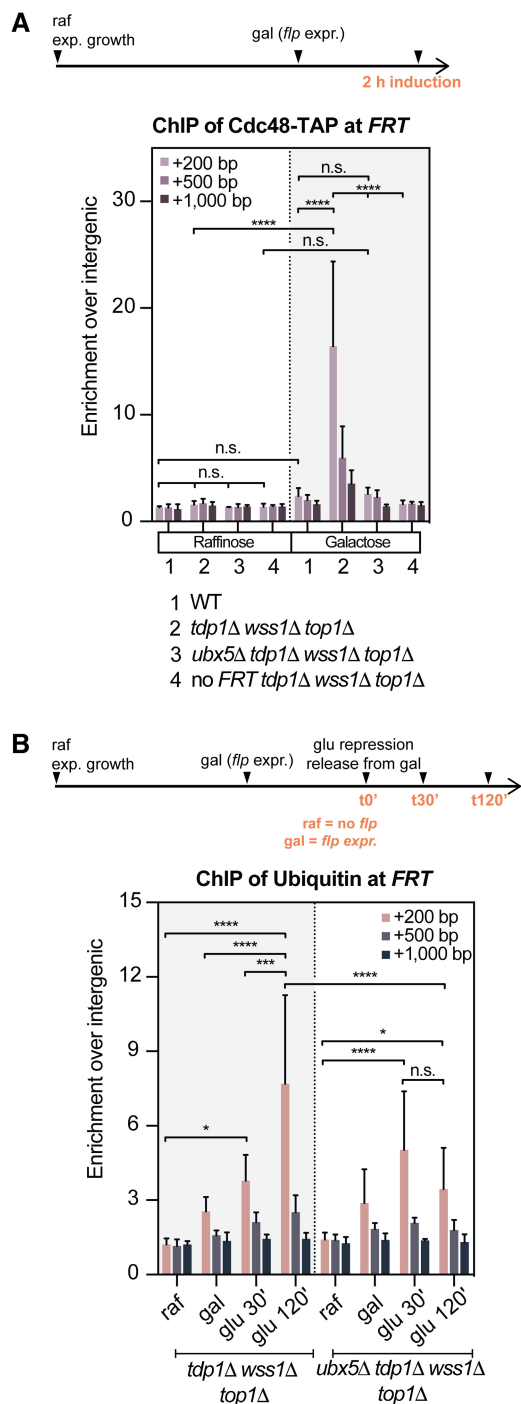
A Schematic representation of the “Flp-nick” system initially described in (Nielsen et al, 2009). The mutant *flp-H305L* recombinase is expressed from a galactose-inducible promoter and targeted to the Flp Recognition Target (*FRT*) site introduced in the yeast genome next to *ARS607*, on chromosome VI. *FRT* consists of three DNA elements (orange) recognized by the Flp recombinase. The location of qPCR primers used for all subsequent ChIP-qPCR analyses is indicated in black, at +200 bp, +500 bp, and +1,000 bp from the *FRT*.

B The *ubx5Δ* mutation rescues growth defects caused by Flp-nick galactose-induction in the *tdp1Δ wss1Δ top1Δ* mutant. Indicated strains were grown in YEP-2% raffinose prior to plating on YEP-2% glucose or YEP-2% galactose plates. Plates were incubated for 3 days at 30°C.

C Cell cycle progression of Flp-nick strains and time points used in (D), monitored by fluorescence-activated cell sorting (FACS). ns, non-synchronized; α -f, alpha-factor; gal, galactose; raf, raffinose.

D *flp-H305L-3HA* dynamics at the *FRT* site in different mutants. Cells were grown in 2% raffinose (raf), synchronized in G1 with alpha-factor (α -f) during induction of *flp-H305L* expression with 3% galactose (gal). Induction was stopped by addition of glucose (glu), and cells were released into the cell cycle. Samples were collected at the indicated time points. Levels of *flp-H305L-3HA* at the *FRT* locus were assessed by ChIP and qPCR without formaldehyde crosslinking. The positions of qPCR primers +200 bp, +500 bp, and +1,000 bp downstream of *FRT* are indicated in (A). Data are presented as the percentage of input showing the means \pm SDs for $n = 5$ independent biological replicates. Significance for +200 bp was defined by ordinary one-way ANOVA using Tukey’s multiple comparison test (n.s., non-significant; * $P < 0.05$; ** $P < 0.01$; *** $P < 0.001$). No *FRT* binding site and no *flp-H305L-3HA* expression (raf) were used as negative controls. See (C) for cell cycle analyses by FACS.

E Ubx5 occupancy at the Flp-bound *FRT* site. Levels of Ubx5-TAP were monitored by ChIP and qPCR following formaldehyde crosslinking in cells grown as described in (D). The graph shows enrichment of qPCR signals over the unrelated intergenic region. Data are presented as means \pm SDs for $n = 5$ independent biological replicates. P -values for +200 bp were defined by 2-way ANOVA using Tukey’s multiple comparisons test (n.s., non-significant; * $P < 0.05$; ** $P < 0.01$; **** $P < 0.0001$). In addition to the indicated mutations, all strains are *bar1Δ* Ubx5-TAP. No *FRT* strain and raffinose (raf) samples were used as negative controls.



in *ubx5Δ*-mediated suppression of *tdp1Δ wss1Δ* and *wss1Δ* hypersensitivity to DPC-inducing drugs, probably by mediating proteolytic digestion of the DPC. Indeed, this last point is demonstrated by the inability of the Ddi1 catalytic mutant (D220A; Fig 5F) to restore DPC-inducing drugs resistance when introduced into *ubx5Δ wss1Δ* (Fig 5G). As it was previously reported, the *ddi1-D220A* mutant induces phenotypes similar to *ddi1Δ*. Overall, these results indicate that Ddi1 provides resistance to DPC-inducing drugs in cells lacking Ubx5 and Wss1.

Figure 4. Cdc48 recruitment at crosslinked Flp depends on Ubx5.

A Cdc48 occupancy at the Flp-bound *FRT* site. Levels of Cdc48-TAP were monitored by ChIP and qPCR following formaldehyde crosslinking in asynchronous cells before and after Flp-cc induction with galactose. The graph shows enrichment of qPCR signal over the unrelated intergenic region. Data are presented as means \pm SDs of three to four independent biological replicates. *P*-values for +200 bp were defined by 2-way ANOVA using Tukey's multiple comparisons test (n.s., non-significant; *****P* < 0.0001). In addition to the indicated mutations, all strains are Cdc48-TAP. No *FRT* strain was used as a negative control.

B Ubiquitination of the *FRT* locus. Asynchronous cultures were grown in 2% raffinose (raf) or additionally supplemented with 3% galactose (gal) to induce *flp-H305L* expression. Cells were also collected during glucose repression of *flp-H305L* expression at time points 30 min (glu 30') and 120 min (glu 120'). Ubiquitin antibody was used for ChIP-qPCR analysis following formaldehyde crosslinking. Data are shown as the mean \pm SDs of three to six independent biological replicates. *P*-values for +200 bp were defined by 2-way ANOVA using Tukey's multiple comparisons test (n.s., non-significant; **P* < 0.05; ****P* < 0.001; *****P* < 0.0001). In addition to all indicated mutations, all strains are *bar1Δ Ddi1-TAP*.

Ubx5 prevents efficient turnover of stalled RNAPII in the absence of Wss1

Several studies have revealed that the largest subunit of RNAPII, Rpb1, is prone to stalling and degradation after exposure to genotoxic agents (Beaudenon *et al*, 1999; Malik *et al*, 2008; Verma *et al*, 2011; Wilson *et al*, 2013). The UV-induced degradation of Rpb1 depends on Cdc48, as well as its cofactor proteins Ubx4 and Ubx5 (Verma *et al*, 2011). Albeit DNA-bound Rpb1 is currently not shown to be a DPC, its degradation after UV or HU exposure still engages the DPC-proteases Ddi1 and Wss1 (Serbyn *et al*, 2020). It is still unclear how Ddi1 and Wss1 may assist Ubx4-Ubx5-Cdc48 in the extraction of stalled Rpb1, but it is likely that stalled Rpb1 is a substrate of these two proteases.

In light of the suppressing effect of *ubx5Δ* on *wss1Δ* cells and the requirement of Ddi1 in this context, we aimed to assess how Rpb1 stability was altered in these conditions. We evaluated Rpb1 protein levels in total yeast cell extracts following HU treatment. As formerly reported, Rpb1 was rapidly degraded in response to HU exposure in WT cells, while loss of Ubx5 or Wss1 hindered this process (Fig 6A and B). Surprisingly, the double *ubx5Δ wss1Δ* mutant was proficient for Rpb1 turnover, although both proteins alone are strictly required for degradation. Additionally, Rpb1 turnover in *ubx5Δ wss1Δ* was dependent on Ddi1 (Fig 6A and B). These observations reveal that the function of Wss1 in Rpb1 degradation can be bypassed if *UBX5* is deleted, strongly favoring the Ddi1-dependent pathway.

With respect to prior work that described Rpb1 accumulation on chromatin in *wss1Δ* (Serbyn *et al*, 2020), we also examined DNA-bound Rpb1 in the mutants generated in this study. Consistently, Rpb1 accumulation can easily be observed in *wss1Δ* (Fig 6C, lane 2; Fig 6D), and this stabilization is counteracted in *ubx5Δ wss1Δ* (Fig 6C, lane 4). Finally, Rpb1 was highly abundant on chromatin in the triple mutant *ubx5Δ wss1Δ ddi1Δ* (Fig 6C, lane 5; Fig 6D), emphasizing the importance of Ddi1 in the suppressing effect of *ubx5Δ*. Taken together, these data suggest that Ubx5 contribution to the clearance of stalled DNA-bound Rpb1 is relevant only in the presence of Wss1. This argues that Wss1 and Ubx5 may cooperate

for genotoxin-induced Rpb1 turnover. When Wss1 and Ubx5 are lost, the pathway for degradation of stalled RNAPII is compromised and strongly relies on Ddi1.

Discussion

With the progression of studies on DNA-protein crosslinks, several repair routes have been discovered but the contribution of each pathway still needs to be elucidated. This study aimed to gain a deeper understanding of the involvement of the AAA ATPase Cdc48 in the cellular response to DPCs. Here, we show that the UBX protein Ubx5 is the major Cdc48 adaptor capable of suppressing the phenotype associated with the defective Wss1-dependent route of proteolytic DPC processing. Interruption of Ubx5-Cdc48 interaction was sufficient to abrogate phenotypes linked to loss of Wss1 or deletion of both critical Top1cc repair genes *WSS1* and *TDP1*. Our data indicate that Ubx5 is targeted to DPC sites and prevents them from proteolysis if Wss1 enzymatic activity is unavailable. Moreover, Wss1 cannot efficiently perform its proteolytic activity without prior action of Ubx5-Cdc48, revealing an unexpected role of Ubx5 in coordinating the cooperation between Cdc48 and Wss1 in the removal of DNA-bound proteins. We exploit these observations to propose a model for Ubx5-Cdc48 and Wss1 co-action in DPC elimination (Fig 7), in which Ubx5 targets Cdc48-Ufd1-Npl4 to ubiquitinated DPCs for initial processing of the protein adduct, followed by Wss1 recruitment to complete proteolysis.

Ubx5 targets Cdc48 and assists Wss1 at DNA-bound proteins

An unexpected finding from our work is that cells deprived of Ubx5-Wss1 are resistant to DPCs (Fig 2A) and present a normal Rpb1 turnover following exposure to HU (Fig 6A and B), although both Ubx5 and Wss1 activities are important to mediate extraction of Rpb1 from chromatin (Fig 6C and D; Verma *et al*, 2011; Serbyn *et al*, 2020). Given the established connection between SPRTN/Wss1 and p97/Cdc48 in several reports (Davis *et al*, 2012; Ghosal *et al*, 2012; Mosbech *et al*, 2012; Stingle *et al*, 2014; Balakirev *et al*, 2015; Fielden *et al*, 2020; Kroning *et al*, 2022), we suggest that the protease Wss1 is assisted by the unfolding activity of Ubx5-Cdc48 to remove chromatin-bound proteins. It remains to be elucidated which comes first, Wss1 or Cdc48? On one hand, Cdc48 might extract by-products generated by Wss1 enzymatic activity. On the other hand, the activity of Cdc48 may be required to prepare the DPC and facilitate its proteolysis by Wss1.

For several reasons, we envision that Ubx5-Cdc48 is targeted before Wss1. In support of this hypothesis, we were able to detect a substantial accumulation of both Ubx5 and Cdc48 at a Top1cc-like locus, especially in the absence of Wss1 (Figs 3E and 4A). Experiments in human cells showed that p97/Cdc48 enabled proteolysis of TOP1cc by SPRTN/Wss1, probably by unfolding the adduct to increase accessibility for SPRTN cleavage (Fielden *et al*, 2020). Overall, the data support a model in which Ubx5-Cdc48 engaged on a crosslinked protein is unable to complete substrate degradation without Wss1. Consequently, in the absence of Wss1, Ubx5-Cdc48 is targeting and masking the DNA-bound protein (Figs 3E and 4A), which will prevent easy access to parallel repair factors, such as Ddi1 (Fig 5). In this view, we propose that if Ubx5-Cdc48 is unavailable, the function of Wss1 would

be partially compromised as the initial processing and unfolding of the adduct would not occur (Fig 7). Despite our efforts, we could not detect Wss1 at DPCs, and our view of the recruitment of Wss1 to DPCs strongly relies on genetic data.

Is Ubx5-Cdc48 strictly required for Wss1 enzymatic activity on DPCs?

Our data showing that *ubx5Δ* mutant cells are not sensitive to DPCs induced by FA, HU (Fig 2A), or CPT (Figs EV2A and EV3C) argue against the above-mentioned model. However, it can also suggest that, although Ubx5 is crucial for turnover of some DNA-bound proteins following exposure to genotoxins (Fig 6A and B), it may be dispensable for removal of other types of adducts potentially targeted by Wss1. This statement is supported by some recent *in vitro* experiments. Using biochemical reconstitution of purified proteins, the authors revealed that SPRTN/Wss1 is sufficient for proteolysis of loosely folded DPCs, but p97/Cdc48 is required for proteolytic cleavage of tightly folded DPCs (Kroning *et al*, 2022). One could therefore propose that the reliance on Ubx5-Cdc48 unfolding activity depends on the structural characteristics of the DPC encountered. Thus, if Ubx5-Cdc48 is engaged on tightly folded DPCs, it might absolutely require Wss1's activity to finalize the extraction, which is demonstrated in our experiments by a great accumulation of both Ubx5 and Cdc48 at DPCs in the absence of Wss1 (Figs 3E and 4A). As shown by *ubx5Δ* which alleviates *wss1Δ* phenotypes (Fig 2A), Wss1 could be assisted by Ubx5-Cdc48 in a wide variety of DPCs, whereas the protease may absolutely rely on Ubx5-Cdc48 unfolding activity only for a specific subset of tightly folded DPCs. This model also partially explains why *wss1Δ* mutant cells complemented with a Wss1 allele deficient in Cdc48 binding are resistant to HU exposure (Maddi *et al*, 2020), but not to Top1-crosslink accumulation (Stingle *et al*, 2014). In the same line, the mammalian SPRTN-SHP mutant allele deficient in p97 binding is not processive in the repair of TOP1ccs (Fielden *et al*, 2020).

Alternatively, in the absence of Ubx5-Cdc48, Wss1 may eventually still be able to process DPCs, but in a longer time frame. A recent study highlighted that p97-UFD1-NPL4 activity has a high ubiquitin threshold (Deegan *et al*, 2020; Fujisawa *et al*, 2022) and that mammalian UBXD7 (Ubx5 homolog) reduces it (Fujisawa *et al*, 2022). It is proposed that UBXD7 promotes the formation of productive p97-UFD1-NPL4 complexes on chains of only five ubiquitins. Yet, absence of UBXD7 does not hinder the efficiency of p97-UFD1-NPL4 on longer ubiquitin chains. It is conceivable to attribute a similar function to yeast Ubx5-Cdc48 in DPC processing, by promoting Wss1 recruitment or activity toward substrates with short ubiquitinated substrates. This could explain why both Ubx5 and Cdc48 are not detected in WT-like condition on a DPC, as they may promote efficient removal (Figs 3E and 4A). In this model, the absence of Ubx5-Cdc48 complex does not necessarily prevent Wss1 targeting and activity. However, once Ubx5-Cdc48 is engaged, it relies on the protease for efficient repair. Additional investigation is required to reveal the extent to which Wss1 relies on Ubx5-Cdc48 complex.

Ddi1 as an alternative pathway for deficient Wss1

Although Wss1 may be the primary response to DPCs, an excess of DPCs could saturate this pathway and cells may require alternative

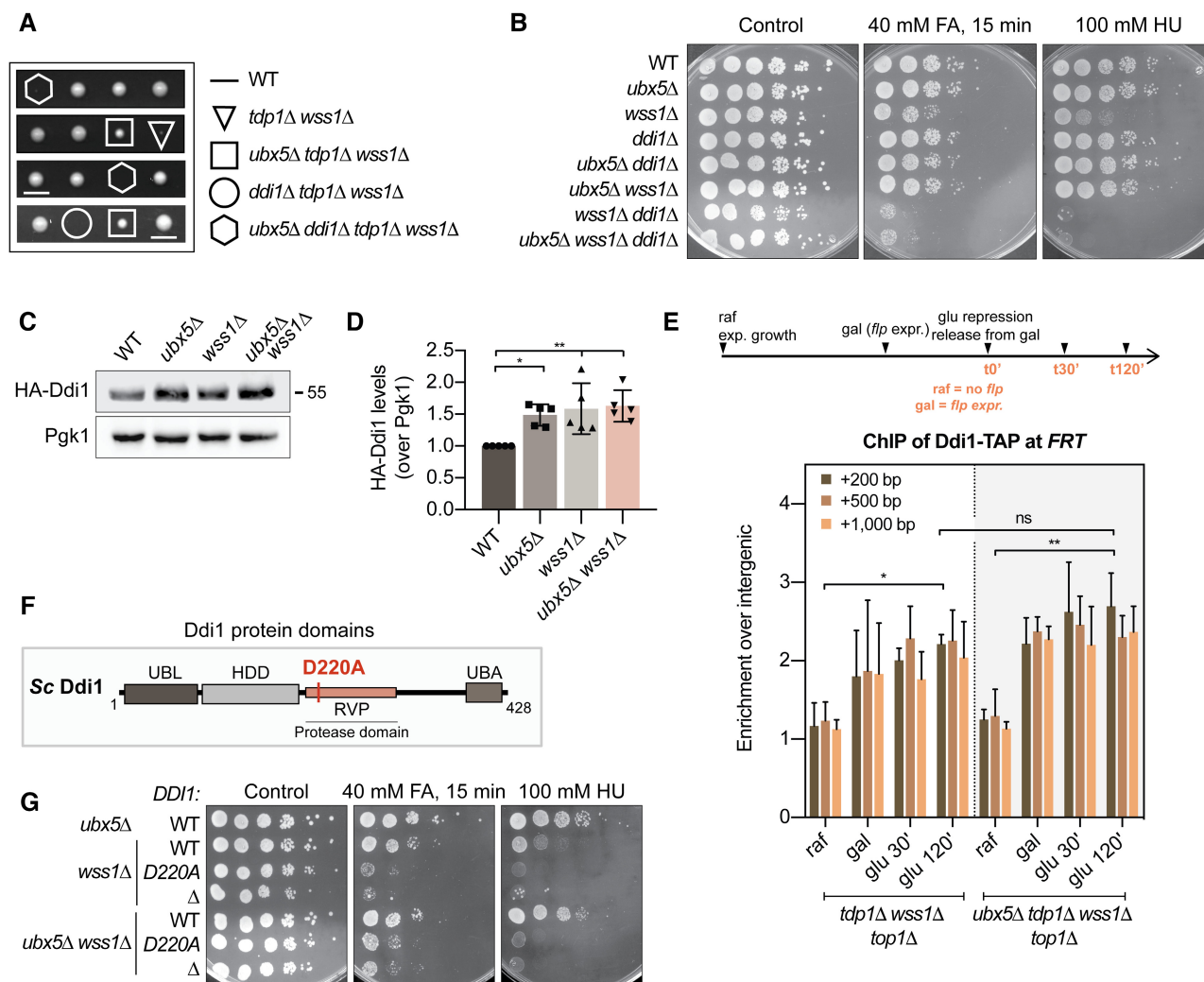


Figure 5. The suppressing effect of *ubx5Δ* partially depends on the protease Ddi1.

- A The suppressing effect of *ubx5Δ* in *tdp1Δ wss1Δ* depends on the ubiquitin-dependent protease Ddi1. Tetrads were analyzed after dissection of the diploid (*TDP1/wss1Δ; WSS1/wss1Δ; UBX5/ubx5Δ; DDI1/ddi1Δ*).
- B *ubx5Δ* restores *wss1Δ* resistance to HU and FA but not upon additional deletion of *DDI1*. Strains were grown in YEPD and either treated with 40 mM FA for 15 min or directly spotted on plates containing 100 mM of HU or 5 μ g/ml CPT. Plates were incubated for 2 days at 30°C.
- C Endogenous HA-Ddi1 levels are still elevated upon additional *ubx5Δ* mutation. Levels in total cell extracts were compared by immunoblotting. For quantification, anti-HA signal was normalized to Pgk1 and then normalized to WT (see (D)).
- D Quantification of HA-Ddi1 levels shown in (C). The anti-HA signal was compared to Pgk1 and normalized to WT. Quantifications of five biological replicates are presented as means \pm SDs. Significance was defined by ordinary one-way ANOVA using Dunnett's multiple comparisons test and WT as a control (* $P < 0.05$; ** $P < 0.01$).
- E Ddi1 occupancy at the *FRT* site. Levels of Ddi1-TAP were examined by ChIP-qPCR following formaldehyde crosslinking. Cells were grown as explained in legend of Fig 4B, and collected at the indicated time points. The enrichments relative to intergenic were plotted as means \pm SDs of three independent biological replicates. *P*-values for +200 bp were defined by 2-way ANOVA using Tukey's multiple comparisons test (n.s., non-significant; * $P < 0.05$; ** $P < 0.01$). In addition to the indicated mutations, all strains are *bar1Δ* Ddi1-TAP.
- F Scheme of Ddi1 protein and catalytic residue D220. When mutated, the *ddi1-D220A* mutant is catalytically inactive.
- G Catalytic activity of the protease Ddi1 is essential for survival of the *ubx5Δ wss1Δ* yeast mutant. Mutants carrying wild-type (WT) Ddi1, D220A catalytic mutant or *ddi1Δ* in combination with *ubx5Δ, wss1Δ*, or double *ubx5Δ wss1Δ* were grown in YEPD. Cells were treated with 40 mM formaldehyde (FA) for 15 min or directly spotted on plates supplemented with 100 mM hydroxyurea (HU). Plates were incubated for 2 days at 30°C.

repair pathways, such as Ddi1. However, if Ubx5-Cdc48 is targeted first, it requires Wss1 to finalize adduct proteolysis, as proposed in the previous paragraph. Consequently, this may result in a slow disassociation of Ubx5-Cdc48 from the DNA-bound adduct in *wss1Δ*, which would compete with other repair factors for the access to the

lesion and therefore be lethal. Supporting our model, a previous study performed in mammalian cells suggested that UBXD7 (Ubx5 homolog) was shielding substrates to protect them from proteasomal factors, leaving them for p97-dependent processing (Alexandru et al, 2008). Consequently, the use of p97-inhibitor induces

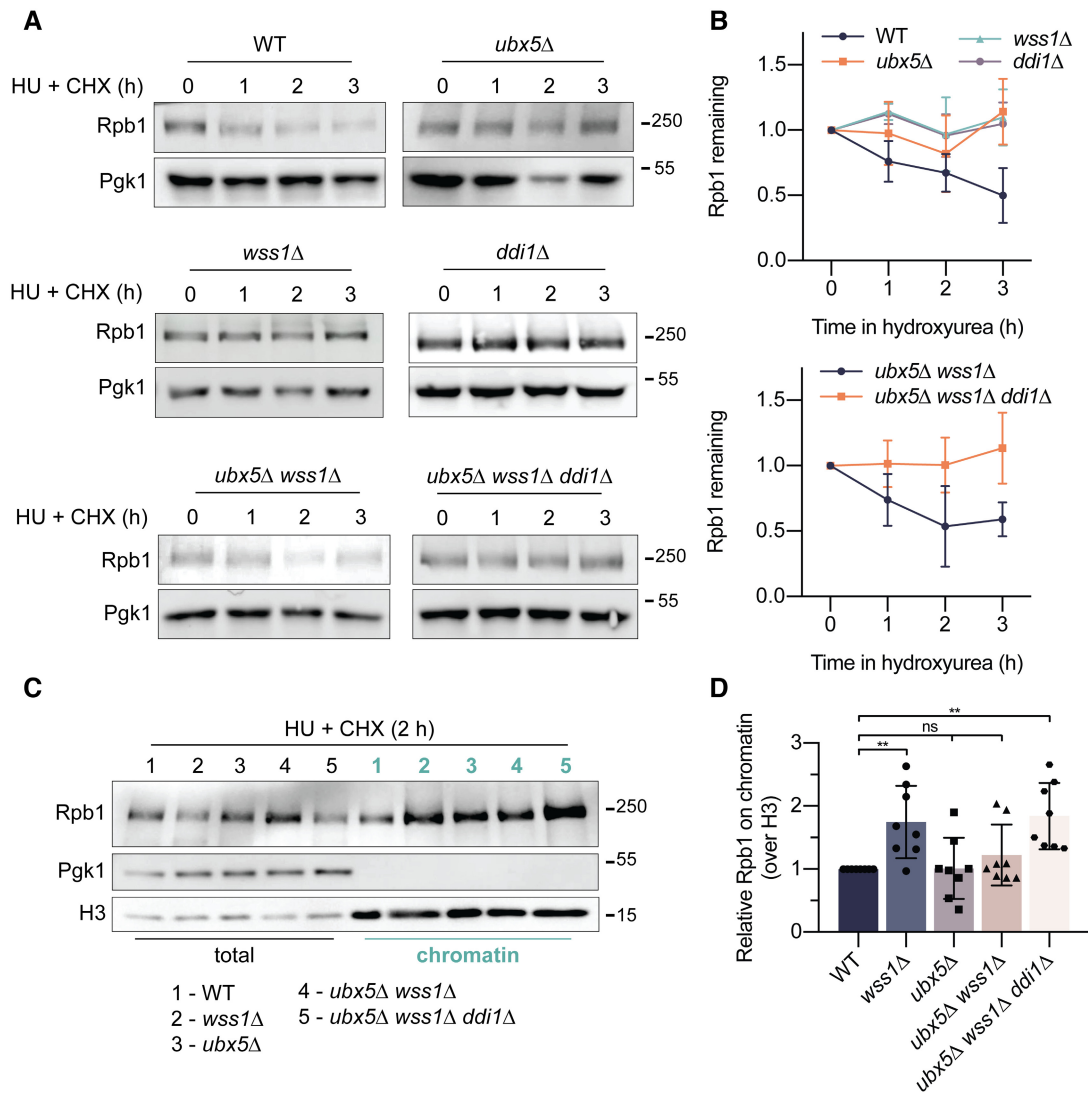


Figure 6. Ubx5 loss promotes Rpb1 degradation in the absence of the DPC protease Wss1.

A Ubx5 loss restores HU-induced Rpb1 degradation in *wss1Δ* and requires Ddi1. Rpb1 levels were defined in cells growing in the presence of 200 mM HU and 100 μ g/ml cycloheximide (CHX) at the indicated time points. Rpb1 and Pgk1 levels in total cell extracts were probed by immunoblotting and quantified using fluorescent secondary antibodies. See (B) for quantifications. Images show immunoblotting using chemiluminescence.

B Rpb1 turnover representative of pictures shown in (A). Relative Rpb1 to Pgk1 levels were set to 1 in the respective non-treated samples. Graphs show values of means \pm SDs of three to six independent biological replicates.

C, D Rpb1 chromatin enrichment following HU treatment. (C) Chromatin fractions were isolated from cells treated for 2 h with 200 mM HU and 100 μ g/ml CHX. Pgk1 and H3 were used as controls to monitor the fractionation. (D) Quantifications of Rpb1 and H3 levels in chromatin fractions. Relative Rpb1 to H3 levels were set to 1 in the respective WT samples. Quantifications of eight biological replicates are presented as means \pm SDs. Significance was defined by ordinary one-way ANOVA using Dunnett's multiple comparison test and WT as a control (n.s., non-significant; ** $P < 0.01$).

trapping of UBXD7 on substrates, while absence of UBXD7 leaves the substrate accessible for engaging proteasome factors.

In agreement with this idea, we observed a substantial accumulation of both Ubx5 and Cdc48 at the Flp-cc in the absence of Wss1 and Tdp1 (Figs 3E and 4A). In addition, ubiquitin and Ddi1 levels detected at the Flp-cc remained high upon Ubx5 deletion, although DPCs were processed (Figs 3D, 4B, and 5C–E). Indeed, the amount of DPC is lower in *ubx5Δ tdp1Δ wss1Δ* compared to *tdp1Δ wss1Δ*. These data suggest that the activity of Ddi1, or its access to Flp-cc

may be inhibited by a prolonged association of Ubx5-Cdc48 on the lesion. More to that, Ddi1 requires very long ubiquitin chains (Yip et al, 2020). It is therefore tempting to speculate that accumulation of Ubx5-Cdc48 may block the growth of ubiquitin chains. Consequently, lack of Ubx5 may allow faster growth of long ubiquitin chains and, accordingly, efficient recruitment and proteolysis by Ddi1. In line with this idea, the catalytic activity of Ddi1 remains essential for cellular resistance of the *ubx5Δ wss1Δ* mutant towards DPCs and DNA-bound proteins (Figs 5F and G, and 6).

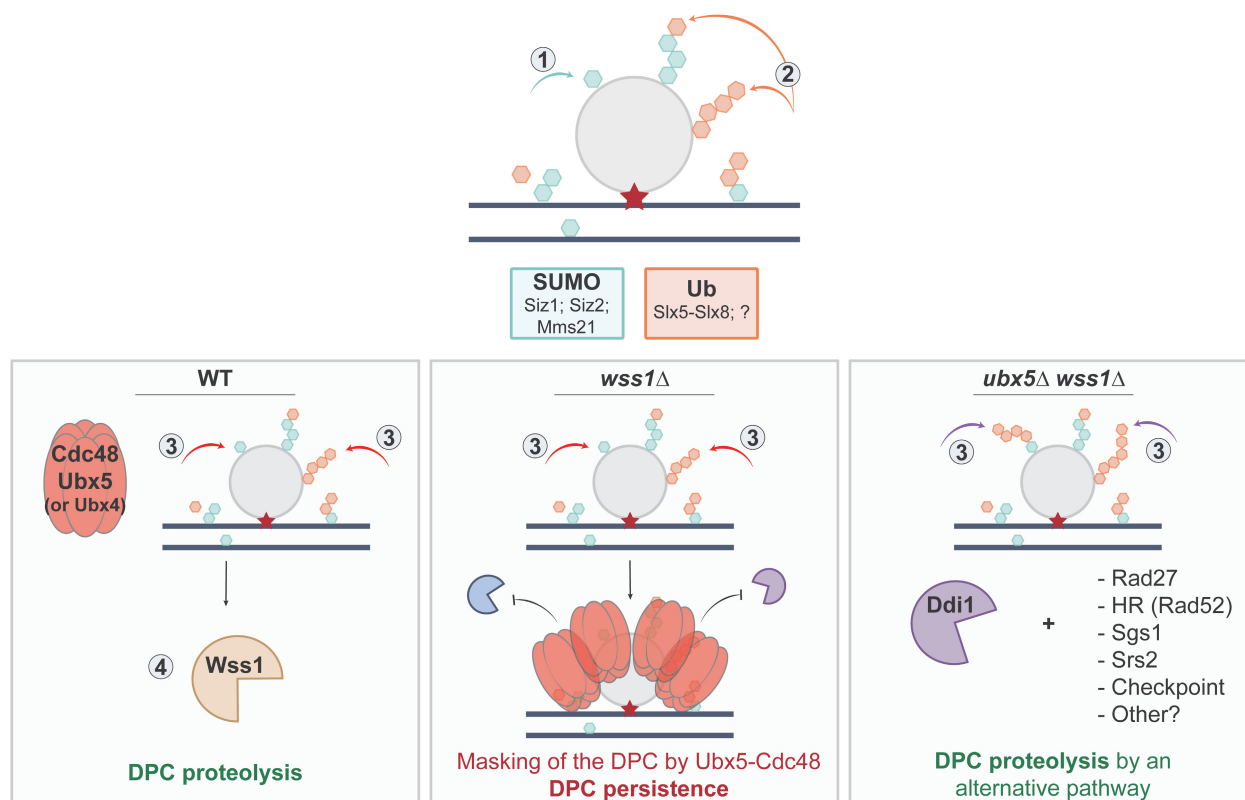


Figure 7. Putative model for Ubx5-Cdc48 in DPC repair.

Repair of a DPC (Top1cc, Flp-cc, stalled Rpb1, etc.) in budding yeast *S. cerevisiae*. Persistence of the protein adduct on chromatin results in sumoylation (SUMO; by Siz1, Siz2, or Mms21 E3 ligases) and ubiquitylation (Ub; by Slx5-Slx8 and potentially other E3 ligases), allowing Ubx5-Cdc48-Ufd1-Npl4 loading and initial remodeling of the protein adduct. Proper protein extraction is ensured by the additional recruitment of the protease Wss1. In the absence of Ubx5-Cdc48-Ufd1-Npl4, Wss1 may still be able to initiate the proteolysis (not shown).

If Wss1 is unavailable (*wss1Δ*), Ubx5-Cdc48 is still targeted to the DPC site, but the proteolysis is not efficient enough to open access for Tdp1 or other endonucleases, and one or several Ubx5-Cdc48 complexes mask the damage site. Accumulation of Ubx5-Cdc48 prevents access to other salvage pathways. Loss of Ubx5 (*ubx5Δ wss1Δ*), or abrogation of its interaction with Cdc48, allows access to the DPC lesion site for alternative repair pathways, which may involve the DPC proteases Ddi1 and 26S proteasome, as well as other canonical repair pathways.

While we propose that ubiquitination is a platform for the recruitment of Ubx5-Cdc48-Wss1 and the protease Ddi1 to DPCs, it should not be neglected that other cellular mechanisms rely on ubiquitination as well. For example, previous studies shed light on the importance of the proteasome in ubiquitin-dependent DPC degradation (Borgermann *et al.*, 2019; Larsen *et al.*, 2019; Sparks *et al.*, 2019; Sun *et al.*, 2020a). Although we detected the ubiquitin signal in close vicinity to the Flp-cc (Fig 4B, + 200 bp), it remains unclear whether the modification is placed on the DPC itself, or involves other proteins.

Homologous recombination and nucleotide excision repair in DPC repair

In previously published findings, a synthetic lethality interaction was reported between yeast Wss1 and Rad52-dependent HR pathway (Stinglele *et al.*, 2014). A similar interplay was found in mammalian cells depleted of BRCA2-dependent HR and SPRTN (Ruggiano *et al.*, 2021). In support of these findings, our results show that HR is

critical for yeast cell survival in the absence of Ubx5, Tdp1, and Wss1 (Fig EV4B), suggesting that HR-dependent processing of DPCs acts in parallel to Wss1. Loss of Ubx5 may allow the action of other activities, such as HR, to compensate for the absence of Wss1 and Tdp1.

We extensively used the Flp-nick system and showed that Ubx5 was consistently enriched at the *FRT* site in the absence of Wss1 (Fig 3E). Interestingly, microscopy experiments revealed the presence of the HR component Rad52 at the *FRT* site (Nielsen *et al.*, 2009). Therefore, Ubx5 may not only prevent the access of repair factors such as Ddi1 to Flp-cc, but also restrict the accessibility of HR factors.

Previous studies have investigated the contribution of the NER pathway in the elimination of DPCs (Reardon & Sancar, 2006; Baker *et al.*, 2007; de Graaf *et al.*, 2009; Nakano *et al.*, 2007, 2009; Stinglele *et al.*, 2014), and a synthetic lethality interaction was identified between yeast Wss1 and NER (Stinglele *et al.*, 2014). However, our genetic analyses challenge these observations. Our data indicate that the Ubx5-mediated suppression of DPC repair-deficient strains does

not rely on NER (Fig EV5C). Yeast cells depleted of Wss1, Tdp1, and NER are viable in the absence of Ubx5 (Fig EV5C). In the context of Ubx5-suppression, NER appears to play a minor role compared to other pathways, such as HR or proteolytic digestion by Ddi1.

Our study assessed the relationship between Ubx5, Wss1, and other repair mechanisms only in unstressed conditions (Figs EV4 and EV5), whereas the synthetic lethality phenotype of Wss1 and NER-deficient strains was observed after treatment with FA (Stingele et al, 2014). Therefore, a viable *ubx5Δ tdp1Δ wss1Δ* mutant depleted of NER may exhibit acute sensitivity to FA-induced DPCs. Although our observations are contradictory to some published reports, they are consistent with other studies that attributed a minor role to NER in repairing DPCs (Quievryn & Zhitkovich, 2000; de Graaf et al, 2009; Nakano et al, 2007, 2009; Zecevic et al, 2010). Understanding the exact contribution of these pathways in yeast will require additional work.

Cdc48 uses different adaptors to target different DPC types

The large variety of Cdc48 adaptors raises the question of how many can act in DPC repair pathways and whether they are redundant. Indeed, Cdc48/p97 can associate with its adaptors in different ways to form various assemblies (Alexandru et al, 2008; Schubert & Buchberger, 2008; Buchberger et al, 2015); Cdc48/p97 can also bind cofactors in a hierarchical manner to provide additional substrate specificity (Hanzelmann et al, 2011). For instance, the mammalian UBXD7 protein only binds to p97 in complex with UFD1-NPL4 and not to p97 alone (Hanzelmann et al, 2011). It is therefore not surprising to find both Ufd1 and Npl4 as suppressors of the *tdp1Δ wss1Δ* mutant along with Ubx5, despite the essentiality of the *UFD1* gene (Fig 1A), supporting a model in which Cdc48 recruitment to DPCs is toxic in this cellular context.

Similarly, SPRTN/Wss1 interacts specifically with p97/Cdc48 bound to UFD1-NPL4 (Davis et al, 2012). These data raise the possibility that Ubx5 acts in DPC repair specifically along with Cdc48-Ufd1-Npl4. In human cells, the p97/Cdc48 adaptor TEX264 is strictly required for SPRTN-mediated repair of TOP1ccs (Fielden et al, 2020) and is so far restricted to TOP1cc processing. Likewise, Ubx5 could be implicated in a specialized complex required for repair of a subtype of DPCs in yeast.

Among the UBX protein family, Ubx4 also turned out to be an interesting suppressor of *tdp1Δ wss1Δ* (Figs 1A and EV3A and B). Given that Ubx4 and Ubx5 are redundant and in charge of a similar function in RNAPII turnover following UV damage (Verma et al, 2011), one could hypothesize a redundant role for Ubx4 and Ubx5 in DPC repair as well. This could provide another explanation for why *ubx5Δ* shows no sensitivity toward DPC-inducing agents (Figs 2A, EV2A, and EV3C), as Ubx4 could take over its role. However, a double *ubx4Δ ubx5Δ* mutant is not sensitive to DPCs induced by several drugs (Fig EV3C and D), arguing against this proposal. One could speculate that in the case of Top1cc, Tdp1 may still be taking care of the repair and this could explain the absence of a phenotype for the *ubx4Δ ubx5Δ* mutant. For instance, Top1cc-sensitivity of yeast cells can be revealed only by simultaneous depletion of Wss1 and Tdp1 (Stingele et al, 2014). However, additional deletion of *TDPI* in *ubx4Δ ubx5Δ* did not change CPT resistance (Fig EV3D). As proposed above, the activity of Wss1 may not strictly depend on UBX

proteins interacting with Cdc48, providing a partial answer to this lack of additivity.

In contrast, *ubx5Δ* completely abolished Cdc48 accumulation at a DPC site in *tdp1Δ wss1Δ* (Fig 4A), suggesting that the segregase is not targeted by other cofactors in the context of Flp-cc. Yet, our data do not exclude the possibility of distinct substrate specificities for Ubx4 and Ubx5 in DPC repair. Ubx5 is perhaps the major substrate targeting adaptor for Cdc48 regarding Top1ccs, but we do not exclude the role of other Cdc48 cofactors can have in DPC repair. In favor of this explanation, it was previously reported that Ubx5 is one of the UBX proteins that binds the most strongly to Cdc48, while Ubx4 has a weak binding (Schubert et al, 2004). Consequently, other Cdc48 cofactors may be involved in DPC repair along with Wss1, that we might not be able to reveal with our genetic approach identifying Top1cc repair factors (Fig 1A).

Cdc48 is able to be directed to mixed SUMO-ubiquitin chains, which could trigger the recruitment of the protease Wss1 to these chains (Nie et al, 2012). However, the SUMO-binding capacity of Wss1 remains essential for proteolytic cleavage *in vivo* (Mullen et al, 2010; Stingele et al, 2014; Balakirev et al, 2015). Consistently and given the number of Cdc48 cofactors, Ubx5 could perhaps assist Wss1 in the cleavage of mainly ubiquitinated DPCs, while other cofactors may be required for other types of signals. In mammals, the activity of SPRTN on protein adducts is also dependent on both sumoylation and ubiquitin signals (Ruggiano et al, 2021).

To our surprise, the Cdc48 cofactor Doa1 did not appear as a suppressor of *tdp1Δ wss1Δ* in the transposon screen (Serbyn et al, 2020; Fig 1A). Contrasting this observation, Doa1 was previously shown to work in DPC repair along with Cdc48 and Wss1 in a ternary complex, capable of targeting SUMO substrates (Balakirev et al, 2015), although Doa1 was thought to be ubiquitin specific (Mullally et al, 2006). These conclusions were drawn from precipitation experiments performed without any stress conditions, and the function of Doa1 in DPC repair was not addressed directly. Doa1 may also be involved in the repair of a specific DPC subtype not tested in our study.

Altogether, our observations support the view that Cdc48/p97 assists Wss1/SPRTN in the repair of a wide range of DPCs, depending on the cofactor it is associated to. It remains to be understood how many Cdc48/p97 cofactors have a relevant function in DPC repair biology and in which specific context they are required. Future studies will reveal how Ubx4 and Ubx5, and probably other Cdc48 cofactors, are orchestrated in DPC repair. This work may provide new insights into the resistance associated with TOP1 inhibitors and help in predicting responses to topoisomerases-targeted therapy.

Limitations of the study: the removal of DPCs and stalled RNAPII

We employed *in vivo* Flp-cc and stalled Rpb1 as two different targets of DPC repair and Cdc48 activities. While Flp-cc involves the creation of a covalent linkage between *flp-H305L* and the DNA, it is not the case for stalled Rpb1. However, it is possible that a prolonged stalling of Rpb1 may lead to a DPC-like lesion. For instance, this has been observed for inhibitor-induced trapping of Poly(ADP-ribose) polymerase -1 and -2 (PARP-1 and PARP-2; Murai et al, 2012), which are so tightly bound to DNA that it results in a DPC-like

lesion, or a “pseudo”-DPC (Stingle *et al.*, 2017). Consistently, the repair of DPCs and the degradation of stalled Rpb1 may share similar mechanisms, including Ubx5, Cdc48, and Wss1. However, some

responses may differ. One important and interesting question is whether the degradation of Rpb1 fully follows the same mechanisms used to degrade protein adducts, such as Flp-cc.

Materials and Methods

Reagents and Tools table

Reagent/Resource	Reference or Source	Identifier or Catalog Number
Experimental Models		
<i>S. cerevisiae</i> strains – See Appendix Table S1 for the list of strains	This Study	N/A
<i>E. coli</i> DH5alpha	N/A	N/A
Recombinant DNA		
See Appendix Table S2 for the list of plasmids	This Study	N/A
Antibodies		
Mouse anti-HA (monoclonal, clone 16B12); for WB 1:2,000; for ChIP 1 µg/1 mg protein	Biologend	901502; RRID: AB_2565006
Mouse anti-Ubiquitin (monoclonal, clone FK2); for ChIP 1 µg/1 mg of protein	Calbiochem	ST1200-100UG; RRID: AB_2043482
Mouse anti-Rpb1 (monoclonal, clone 8WG16); for WB 1:5,000	Biologend	664912; RRID: AB_2650945
Mouse anti-Pgk1 (monoclonal, clone 22C5D8); for WB 1:3,000	Abcam	ab113687; RRID: AB_10861977
Rabbit anti-Histone H3 (polyclonal); for WB: 1:2,000	Invitrogen	PA5-16183; RRID: AB_10985434
Fluorescent secondary Goat IRDye 800CW anti-mouse; for WB 1:4,000	LI-COR	926-32210; RRID: AB_621842
Secondary Goat anti-Mouse-HRP; 1:5,000	DAKO	P0447; RRID: AB_2617137
Secondary Goat anti-Rabbit-HRP; 1:5,000	DAKO	P0448; RRID: AB_2617138
Oligonucleotides and sequence-based reagents		
OFS4363_FRT +200bp_forward; 500 nM AAGTTTCGACATGGGCTTCAG	Serbyn <i>et al.</i> (2020)	N/A
OFS4364_FRT +200bp_reverse; 500 nM TCGTTTGAGGACCTTTGAG	Serbyn <i>et al.</i> (2020)	N/A
OFS4365_FRT +500bp_forward; 300 nM CGGGCAGTAGCTCATCAAGT	Serbyn <i>et al.</i> (2020)	N/A
OFS4366_FRT +500bp_reverse; 300 nM CATGAAGAGGGTGAGGAGGA	Serbyn <i>et al.</i> (2020)	N/A
OFS4367_FRT +1kb_forward; 600 nM CAGCCTGATCATTATTCCA	Serbyn <i>et al.</i> (2020)	N/A
OFS4368_FRT +1kb_reverse; 600 nM CGGACATCACAATCTTGAC	Serbyn <i>et al.</i> (2020)	N/A
OFS2788_intergenic_forward; 500 nM TGTTCCCTTAAGAGGTGATGGTGA	Gali <i>et al.</i> (2017)	N/A
OFS2789_intergenic_reverse; 500 nM GTGCCAGTACTTGAAAACC	Gali <i>et al.</i> (2017)	N/A
See Appendix Table S3 for full list of oligonucleotides	This Study	N/A
Chemicals, enzymes and other reagents		
Zymolyase-20T	Amsbio	120491-1
Phusion High-Fidelity DNA Polymerase	Thermo Scientific	F530L
Auxin (3-indoleacetic acid)	Sigma-aldrich	I2886
Camptothecin	Lucerna-Chem	Cat. no 0215973225
Etoposide	Sigma-aldrich	E1383
Hydroxyurea	Bio Basic	HB0528
Formaldehyde	Sigma-aldrich	1.04003
MG132	Enzo Life Sciences	BML-PI102

Reagents and Tools table (continued)

Reagent/Resource	Reference or Source	Identifier or Catalog Number
Cycloheximide	Sigma-Aldrich	C7698
WesternBright ECL HRP substrate	Advansta	K-12045
WesternBright sirius HRP substrate	Advansta	K-12043
cComplete, Mini, EDTA-free Protease Inhibitor Cocktail	Roche	4693159001
NEM (N-Ethylmaleimide)	Thermo Scientific	40526
Dynabeads Protein G for immunoprecipitation	Invitrogen	10009D
Dynabeads Pan Mouse IgG	Invitrogen	11041
Alpha Factor	PRIMM	201307-00007
Glusulase	Perkin Elmer	NEE154001Ea; lot: 2607947
Propidium Iodide	Sigma	P4170
Proteinase K	Carl Roth	7528.3
4X Bolt LDS Sample Buffer	Life Technologies	B0007
RNase A, PureLink	Invitrogen	12091-021; lot: 1772940; 2364671
The Bio-Rad protein assay	Bio-Rad	500-0006
Phire Green Hot Start II PCR Master Mix	Thermo Scientific	F126L
NEBuilder HiFi DNA Assembly Cloning Kit	NEB	E5520
NucleoSpin Gel and PCR Clean-Up	Macherey-Nagel	Cat. No 740609.250
SYBR Select Master Mix for CFX	Applied biosystems	4472942
MinElute PCR Purification Kit	Qiagen	28006
Deposited data		
Unprocessed imaging (immunoblots, spot assays, tetrades) data	This Study	Mendeley data: https://doi.org/10.17632/hzvwpgs7n8.1
Software		
Prism 8.0.1	GraphPad Software, Inc.	RRID: SCR_002798
Kaluza	Beckman Coulter	RRID: SCR_016182
SnapGene 3.2.1	GSL Biotech LLC	RRID: SCR_015052
Other		
MagNA Lyser Instrument	Roche	3358976001
Bioruptor Twin	Diagenode	UCD-400
Gallios 8 colors 2 Lasers Flo Cytometer	Beckman Coulter	B43619
Real-Time PCR Detection System	Bio-Rad	CFX connect and CFX96
0.5 mm Glass Beads	BioSpecProducts	Cat. No 11079105

Methods and Protocols

Yeast strains and growth conditions

All *S. cerevisiae* yeast strains used in this study (listed in Appendix Table S1) were derived from W303 or S288C genetic backgrounds. Genomic mutations were introduced by transformation and verified by colony PCR, phenotypic analyses, and/or sequencing. Epitope insertions were checked by immunoblotting. Other mutants were obtained by standard techniques and tetrad dissection. TAP-tagged strains were obtained from the yeast fusion library (Ghaemmaghami *et al.*, 2003). Oligonucleotides, template plasmid, or DNA used for PCR and transformation are listed in Appendix Tables S2 and S3. Additional details on strain construction are available upon request.

Yeast cells were grown at 30°C in YEP- (1% yeast extract, 2% peptone) or SC- (1.7 g/l yeast nitrogen base; 5 g/l ammonium sulfate; 0.87 g/l dropout mix) liquid media, or grown on plates supplemented with 20 g/l agar. As a source of sugar, 2% glucose, 2% raffinose, or 2–3% galactose was added. Selection for dominant markers was performed on YEPD-based medium (YEP-2% glucose) supplemented with 200 µg/ml G418, 200 µg/ml cloNAT, or 50 µg/ml Hygromycin B.

E. coli strains and growth conditions

DH5α *E. coli* bacterial strains (listed in Appendix Table S2) were grown at 37°C in LB medium or on LB-2% agar plates supplemented with 50 µg/ml of ampicillin for plasmid selection.

Yeast transformation

Five milliliters of exponentially growing cells were resuspended in 80 μ l LiTE buffer (100 mM LiAc; 10 mM Tris pH 7.5; 1 mM EDTA). Thirty eight microliters of cells were mixed with 100 μ g/ml salmon sperm ssDNA, 37.28% PEG4000, and 200 ng DNA to transform (plasmid DNA or purified PCR product). Cells were incubated for 1 h at 30°C and then supplemented with 6% DMSO, and a heat shock was performed for 10 min at 42°C. Cells were plated on selective media and grown for 2–3 days before isolation of single colonies.

Genetic crosses and tetrad dissection

Haploid strains of opposite mating types were mixed and spotted overnight on a YEPD plate at 30°C, to allow mating and diploid construction. Diploids were selected by streaking the mating mixture overnight onto a plate selecting for the diploid genotype. Spore formation was induced by transferring the diploid cells to KAc sporulation medium (20 g/l potassium acetate; 2.2 g/l yeast extract; 0.5 g/l glucose; 0.87 g/l dropout mix; 20 g/l agar; pH 7) for 4–5 days at 30°C. Before tetrad dissection, the ascus cell wall was digested with 0.5 mg/ml Zymolyase (Amsbio, 120491-1) treatment for 5 min at room temperature. Haploid spores from single tetrads were separated with a micromanipulator and grown on a YEPD plate for 3 days at 30°C. The individual phenotype of the dissected spores was determined by replica plating on agar plates containing selective media (various drop-out and drug media).

Construction of recombinant DNA

Recombinant plasmid DNA was constructed using NEB Builder HiFi DNA Assembly Cloning Kit (NEB, E5520). PCR templates and oligonucleotides used to generate products are provided in Appendix Tables S2 and S3, respectively. Additional details on construction are available upon request.

Colony PCR

Genomic mutations were checked by direct resuspension of yeast strains in Phire Green Hot Start II PCR Master Mix (Thermo Scientific, F126L) supplemented with oligonucleotides at 0.5 μ M.

Spot assays

Yeast mutant growth and sensitivities were assessed by spot assay. Cells were grown exponentially in the appropriate medium at 30°C under continuous rotation and diluted to $OD_{600} = 1-1.5$. 10-fold serial dilutions were spotted on agar plates containing the indicated concentrations of auxin, camptothecin (CPT), and hydroxyurea (HU). To treat cells with formaldehyde (FA), 1 ml of yeast culture was incubated with indicated concentrations of FA for 15 min under rotation. Cells were then harvested by centrifugation, washed twice with 1 ml sterile water then diluted and spotted on plates without drugs.

Protein extraction by TCA, Western blotting, and antibodies

Standard TCA extraction was used for analysis of total protein levels. Yeast cultures were fixed with 6.25% of trichloroacetic acid (TCA), kept on ice for 10 min, pelleted by centrifugation at 4,500 g for 10 min, washed twice with 1 ml of 100% acetone, and dried under vacuum. Pellets were resuspended in 100 μ l of Urea Buffer (50 mM Tris-HCl pH 7.5; 5 mM EDTA; 6 M Urea; 1% SDS), mixed with 200 μ l of glass beads, and subjected to bead-beating in a

MagNa Lyser instrument (Roche) 5 times for 45 s at 4°C, 1 min of pause in between. Final solubilization was performed at 65°C for 10 min and centrifugation 10 min at 16,000 g. Addition of 100 μ l sample buffer (3% SDS; 15% Glycerol; 0.1 M Tris pH 6.8; 0.0133% bromophenol blue; 0.95 M 2-mercaptoethanol) and boiled for 10 min. Protein samples were separated by SDS-PAGE and transferred onto nitrocellulose membrane. After transfer, membranes were blocked for 30 min with 5% milk dissolved in TBS-T (150 mM NaCl, 20 mM Tris-HCl, 0.05% Tween, pH 7.4) and incubated with appropriate antibodies indicated in each figure. See the Reagents and Tools table for a list of antibodies used in this study. Signals were revealed with Western Bright ECL HRP (Advansta, K-12045) or Sirius HRP (Advansta, K-12043) substrates.

Flp-nick induction, chromatin immunoprecipitation (ChIP), and quantitative real-time PCR (qPCR)

Induction of the *flp-H305L-3HA* expression was performed as described in (Nielsen et al, 2009). Briefly, yeast cells were grown to log phase in YEP- 2% raffinose (no transcription of the locus). Where indicated, cells were synchronized in G1 with 200 ng/ml α -factor (PRIMM, 201307-00007) for 1.5 h. Induction was performed for 2 h by addition of 3% galactose. Cells were then washed twice with 20 ml cold YEP (no sugar) medium and released into warm YEP-2% glucose (YEPD) medium. One milliliter of cells were collected to monitor cell-cycle progression at desired time points.

Cells were harvested at the different time points by centrifugation at 1,650 g for 3 min, washed twice with cold 1 \times Phosphate Buffer Saline (PBS) and frozen in 2 ml screw-cap tubes. For Ddi1-TAP, Ubx5-TAP, Cdc48-TAP, and Ubiquitin ChIP, cells were fixed before pelleting by addition of 1% formaldehyde (FA) for 15 min at room temperature, then quenched with 250 mM glycine for 5 min, and kept on ice for at least 10 min. All subsequent steps were performed at 4°C. The frozen cells were resuspended in 1 ml of cold FA lysis buffer (50 mM HEPES-KOH, pH 7.5; 140 mM NaCl; 1 mM EDTA; 1% Triton X-100; 0.1% sodium deoxycholate; protease inhibitor cocktail (Roche)) and lysed by bead-beating with 500 μ l of 0.5 mm glass beads with five cycles of 30 s at 6,000 rpm with 1 min pause in between each bead beating cycle, on a MagNa Lyser Instrument (Roche). Lysates were then recovered in a new tube by centrifugation and further spun at 16,000 g for 30 min. Pellets were resuspended in 1 ml of FA lysis buffer and subjected to DNA sonication for 20 cycles of 30 s in a Bioruptor Twin (Diagenode). Following pelleting by 15 min centrifugation at 16,000 g, soluble fractions were transferred to a new tube and protein concentration was measured by Bio-Rad protein assay (500-0006). For each ChIP, 1 mg of protein (1/10 of input transferred in a new tube) was incubated together with 1 μ l of anti-HA antibodies (BioLegend, 901502 anti-HA.11 clone 16B12, for *flp-H305L-3HA* ChIP), or 1 μ l of anti-Ubiquitin antibodies (Calbiochem, ST1200-100UG clone FK2), or 20 μ l of Dynabeads Pan Mouse IgG (Invitrogen, 11041; for Ddi1-TAP, Ubx5-TAP and Cdc48-TAP ChIP) overnight at 4°C with rotation. Prewashed Protein G Dynabeads (Invitrogen, 100009D) were then added for 3 h to recover antibodies. Beads were collected on magnetic stands and washed once with 500 μ l of FA lysis buffer, twice with 500 μ l of FA-500 buffer (50 mM HEPES-KOH, pH 7.5; 500 mM NaCl; 1 mM EDTA; 1% Triton X-100; 0.1% sodium deoxycholate), twice with 500 μ l of Buffer III (10 mM Tris-HCl pH 8; 1 mM EDTA; 250 mM

LiCl; 1% IGEPAL; 1% sodium deoxycholate) and finally once with 500 μ l of TE buffer (50 mM Tris–HCl pH 7.5; 10 mM EDTA). Proteins were eluted twice with 100 μ l of elution buffer B (50 mM Tris–HCl pH 7.5; 1% SDS; 10 mM EDTA) for 8 min at 65°C. Eluted and input samples were incubated for 2 h at 42°C with 0.75 mg/ml Proteinase K (Carl Roth, 7528.3) and decrosslinked at 65°C for at least 12 h. DNA was purified with the MinElute PCR purification kit (Qiagen, 28006) and eluted from the columns twice with 30 μ l of elution buffer from the kit. Real-time qPCRs were then performed using SYBR Select Master Mix (Applied Biosystems, 4472942) with oligonucleotide pairs listed in the Reagents and Tools Table (FRT +200 bp; +500 bp; +1,000 bp or intergenic) and a Real-Time PCR machine (Bio-Rad). Results are presented as percent of input or normalized to the intergenic region.

Cell cycle analysis by flow cytometry analysis (FACS)

For flow cytometry analysis, 1 ml of yeast cells at $OD_{600} = 0.5$ were harvested by centrifugation and resuspended in 70% ethanol allowing storage at 4°C for up to 1–2 weeks. Next, cells were pelleted at 3,500 g for 2 min and washed with 300 μ l of 50 mM sodium citrate (NaCl) pH 7.2. A second centrifugation at 3,500 g for 10 min was performed, and cells were resuspended in 250 μ l NaCl +5 μ l RNase A (Invitrogen, 12091-021) and incubated for 1 h at 37°C. Staining with 25 μ g/ml Propidium Iodide (PI, Sigma, P4170) was performed at 37°C for 1 h. Cells were then sonicated in a Bioruptor Twin (Diagenode) during five cycles of 5 s, before flow cytometry analysis on a Gallios flow cytometer (Beckman Coulter).

Analysis of Rpb1 levels following hydroxyurea treatment

Overnight cultures were diluted to $OD_{600} = 0.2$. When cells reached $OD_{600} = 0.8$, hydroxyurea (HU; Bio Basic, HB0528) was added to a final concentration of 0.2 M along with 100 μ g/ml cycloheximide (Sigma-Aldrich, C7698) to prevent protein synthesis. Cultures collected at different time points were subjected to TCA protein extraction and immunoblotted with anti-Rpb1 (BioLegend, 664912 clone 8WG16) or anti-Pgk1 (Abcam, ab113687 clone 22C5D8) antibodies. Fluorescent secondary antibodies (LI-COR, 926-32210) were used for quantification analyses.

Isolation of chromatin

The protocol was adapted from Kubota *et al* (2012). Fifty OD of yeast cells were harvested by spinning down cultures for 3 min at 1,650 g and washed once with 1 \times cold Phosphate Buffer Saline (PBS) and frozen. Pelleted cells were resuspended in 1 ml of pre-spheroblast buffer (100 mM PIPES/KOH, pH 9.4; 10 mM DTT; 0.1% sodium azide) and incubated for 10 min at room temperature and centrifuged for 3 min at 1,800 g. To induce spheroblast formation, cells were resuspended in 1 ml spheroblast buffer (50 mM KH_2PO_4/K_2HPO_4 , pH 7.4; 0.6 M Sorbitol; 0.1 mM DTT; 0.5 mg/ml Zymolyase, 2% Glusulase) and incubated 30 min at 37°C. Spheroblasts were harvested by centrifugation at 1,800 g for 3 min and washed twice in 1 ml wash buffer (20 mM KH_2PO_4/K_2HPO_4 , pH 6.5; 0.6 M Sorbitol; 1 mM $MgCl_2$; 1 mM DTT; 20 mM β -glycerophosphate; 1 mM PMSF; protease inhibitors (Roche)). Spheroblasts were resuspended in 200 μ l of wash buffer and 1/10 of total cell extract was kept as input. Isolation of nuclei was obtained by overlaying spheroblasts on 1.4 ml 18% Ficoll solution (18% Ficoll; 20 mM KH_2PO_4/K_2HPO_4 , pH 6.5;

1 mM $MgCl_2$; 1 mM DTT; 20 mM β -glycerophosphate; 1 mM PMSF; 0.01% IGEPAL; protease inhibitor (Roche)) and tubes were centrifuged for 5 min at 5,000 g. The supernatant was subjected to a second spin at 5,000 g for 5 min, and a final spin at 16,100 g for 20 min to obtain the nuclei in the pellet. Nuclei were resuspended in 200 μ l of EB-X buffer (50 mM HEPES/KOH, pH 7.5; 100 mM KCl; 2.5 mM $MgCl_2$; 0.1 mM $ZnSO_4$; 2 mM sodium fluoride; 0.5 mM Spermidine; 0.25% Triton X-100; 1 mM DTT; 20 mM β -glycerophosphate; 1 mM PMSF; protease inhibitor cocktail) and lysed for at least 10 min on ice. The entire preparation was then transferred on 500 μ l of EBX-S Buffer (EB-X buffer; 30% sucrose) and spun at 16,000 g for 10 min. Chromatin pellet was gently resuspended in 1 ml EB-X buffer and finally centrifuged at 10,000 g for 2 min. The chromatin was resuspended in 30 μ l of 1.5 \times Bolt LDS Sample Buffer (Life Technologies, B0007) and analyzed by immunoblotting with antibodies indicated on each figure. The quality of the fractionation was controlled by immunoblotting against PGK1 (cytoplasm contamination; Abcam, ab113687 clone 22C5D8) and H3 (chromatin extraction; Invitrogen, Pa5-16183).

Quantification and statistical analysis

Volcano plot from Fig 1A was generated using Prism 8. Gene bodies in Figs 1B and EV3A are defined as the ORF. Statistical details can be found in figure legends. Prism 8 was used to quantify *P*-values and generate graphs. The mean and standard deviation (SD) are reported on the graphs.

Data availability

This paper does not report original code.

Unprocessed imaging data were deposited at Mendeley Data: <https://doi.org/10.17632/hzvwpgs7n8.1>.

Further information and requests for resources and reagent should be direct to the lead contact, Françoise Stutz (francoise.stutz@unige.ch).

Expanded View for this article is available [online](#).

Acknowledgements

We thank iGE3. We thank Helle Ulrich for sharing the parental auxin degran strain; Lotte Bjergbaek for the Flp–nick system and Takeo Usui for the *12gene Δ OHSR* strain. We are grateful for Geraldine Silvano's technical assistance. We thank all the members of the Stutz laboratory for critical reading of the manuscript, comments, suggestions, and discussions. This work was supported by funds from the Swiss National Science Foundation (grants 31003A_153331, 31003A_182344, and 310030_208171 to FS), and the Canton of Geneva. AN is supported by an iGE3 fellowship. Open access funding provided by Universite de Geneve.

Author contributions

Audrey Noireterre: Conceptualization; data curation; formal analysis; validation; investigation; visualization; methodology; writing – original draft; writing – review and editing. **Natalia Serbyn:** Data curation; validation; investigation; methodology; writing – review and editing. **Ivona Bagdiul:** Data curation; validation; investigation; methodology. **Françoise Stutz:** Conceptualization; supervision; funding acquisition; project administration; writing – review and editing.

Disclosure and competing interests statement

The authors declare that they have no conflict of interest.

References

- Alexandru G, Graumann J, Smith GT, Kolawa NJ, Fang R, Deshaies RJ (2008) UBXD7 binds multiple ubiquitin ligases and implicates p97 in HIF1 α turnover. *Cell* 134: 804–816
- Alvaro D, Lisby M, Rothstein R (2007) Genome-wide analysis of Rad52 foci reveals diverse mechanisms impacting recombination. *PLoS Genet* 3: e228
- Baker DJ, Wuenschell G, Xia L, Termini J, Bates SE, Riggs AD, O'Connor TR (2007) Nucleotide excision repair eliminates unique DNA-protein crosslinks from mammalian cells. *J Biol Chem* 282: 22592–22604
- Balakirev MY, Mullally JE, Favier A, Assard N, Sulpice E, Lindsey DF, Rulina AV, Gidrol X, Wilkinson KD (2015) Wss1 metalloprotease partners with Cdc48/Doa1 in processing genotoxic SUMO conjugates. *Elife* 4: e06763
- Beaudenon SL, Huacani MR, Wang G, McDonnell DP, Huibregtse JM (1999) Rsp5 ubiquitin-protein ligase mediates DNA damage-induced degradation of the large subunit of RNA polymerase II in *Saccharomyces cerevisiae*. *Mol Cell Biol* 19: 6972–6979
- den Besten W, Verma R, Kleiger G, Oania RS, Deshaies RJ (2012) NEDD8 links cullin-RING ubiquitin ligase function to the p97 pathway. *Nat Struct Mol Biol* 19: S511–S516
- Borgermann N, Ackermann L, Schwertman P, Hendriks IA, Thijssen K, Liu JC, Lans H, Nielsen ML, Mailand N (2019) SUMOylation promotes protective responses to DNA-protein crosslinks. *EMBO J* 38: e101496
- Buchberger A, Schindelin H, Hanzelmann P (2015) Control of p97 function by cofactor binding. *FEBS Lett* 589: 2578–2589
- Cherry JM, Ball C, Weng S, Juvik G, Schmidt R, Adler C, Dunn B, Dwight S, Riles L, Mortimer RK et al (1997) Genetic and physical maps of *Saccharomyces cerevisiae*. *Nature* 387: 67–73
- Chinen T, Ota Y, Nagumo Y, Masumoto H, Usui T (2011) Construction of multidrug-sensitive yeast with high sporulation efficiency. *Biosci Biotechnol Biochem* 75: 1588–1593
- Davis EJ, Lachaud C, Appleton P, Macartney TJ, Nathke I, Rouse J (2012) DVC1 (C1orf124) recruits the p97 protein segregase to sites of DNA damage. *Nat Struct Mol Biol* 19: 1093–1100
- Debethune L, Kohlhagen G, Grandas A, Pommier Y (2002) Processing of nucleopeptides mimicking the topoisomerase I-DNA covalent complex by tyrosyl-DNA phosphodiesterase. *Nucleic Acids Res* 30: 1198–1204
- Decottignies A, Evain A, Ghislain M (2004) Binding of Cdc48p to a ubiquitin-related UBX domain from novel yeast proteins involved in intracellular proteolysis and sporulation. *Yeast* 21: 127–139
- Deegan TD, Mukherjee PP, Fujisawa R, Polo Rivera C, Labib K (2020) CMG helicase disassembly is controlled by replication fork DNA, replisome components and a ubiquitin threshold. *Elife* 9: e60371
- Deichsel A, Mouysset J, Hoppe T (2009) The ubiquitin-selective chaperone CDC-48/p97, a new player in DNA replication. *Cell Cycle* 8: 185–190
- Deng C, Brown JA, You D, Brown JM (2005) Multiple endonucleases function to repair covalent topoisomerase I complexes in *Saccharomyces cerevisiae*. *Genetics* 170: 591–600
- Dizdaroglu M, Gajewski E, Reddy P, Margolis SA (1989) Structure of a hydroxyl radical induced DNA-protein cross-link involving thymine and tyrosine in nucleohistone. *Biochemistry* 28: 3625–3628
- Fielden J, Ruggiano A, Popovic M, Ramadan K (2018) DNA protein crosslink proteolysis repair: from yeast to premature ageing and cancer in humans. *DNA Repair (Amst)* 71: 198–204
- Fielden J, Wiseman K, Torrecilla I, Li S, Hume S, Chiang SC, Ruggiano A, Narayan Singh A, Freire R, Hassanieh S et al (2020) TEX264 coordinates p97- and SPRTN-mediated resolution of topoisomerase I-DNA adducts. *Nat Commun* 11: 1274
- Frattini C, Villa-Hernandez S, Pellicano G, Jossen R, Katou Y, Shirahige K, Bermejo R (2017) Cohesin ubiquitylation and mobilization facilitate stalled replication fork dynamics. *Mol Cell* 68: 758–772
- Fujisawa R, Polo Rivera C, Labib KPM (2022) Multiple UBX proteins reduce the ubiquitin threshold of the mammalian p97-UFD1-NPL4 unfoldase. *Elife* 11: e76763
- Gali VK, Balint E, Serbyn N, Frittmann O, Stutz F, Unk I (2017) Translesion synthesis DNA polymerase h exhibits a specific RNA extension activity and a transcription-associated function. *Sci Rep* 7: 13055
- Ghaemmaghami S, Huh WK, Bower K, Howson RW, Belle A, Dephoure N, O'Shea EK, Weissman JS (2003) Global analysis of protein expression in yeast. *Nature* 425: 737–741
- Ghosal G, Leung JW, Nair BC, Fong KW, Chen J (2012) Proliferating cell nuclear antigen (PCNA)-binding protein C1orf124 is a regulator of translesion synthesis. *J Biol Chem* 287: 34225–34233
- de Graaf B, Clore A, McCullough AK (2009) Cellular pathways for DNA repair and damage tolerance of formaldehyde-induced DNA-protein crosslinks. *DNA Repair (Amst)* 8: 1207–1214
- Hanzelmann P, Schindelin H (2017) The interplay of cofactor interactions and post-translational modifications in the regulation of the AAA+ ATPase p97. *Front Mol Biosci* 4: 21
- Hanzelmann P, Buchberger A, Schindelin H (2011) Hierarchical binding of cofactors to the AAA ATPase p97. *Structure* 19: 833–843
- Hartmann-Petersen R, Wallace M, Hofmann K, Koch G, Johnsen AH, Hendil KB, Gordon C (2004) The Ubx2 and Ubx3 cofactors direct Cdc48 activity to proteolytic and nonproteolytic ubiquitin-dependent processes. *Curr Biol* 14: 824–828
- He J, Zhu Q, Wani G, Wani AA (2017) UV-induced proteolysis of RNA polymerase II is mediated by VCP/p97 segregase and timely orchestration by Cockayne syndrome B protein. *Oncotarget* 8: 11004–11019
- Husnjak K, Dikic I (2012) Ubiquitin-binding proteins: decoders of ubiquitin-mediated cellular functions. *Annu Rev Biochem* 81: 291–322
- Ide H, Shoukamy MI, Nakano T, Miyamoto-Matsubara M, Salem AM (2011) Repair and biochemical effects of DNA-protein crosslinks. *Mutat Res* 711: 113–122
- Ide H, Nakano T, Salem AMH, Shoukamy MI (2018) DNA-protein cross-links: formidable challenges to maintaining genome integrity. *DNA Repair (Amst)* 71: 190–197
- Jentsch S, Rumpf S (2007) Cdc48 (p97): a “molecular gearbox” in the ubiquitin pathway? *Trends Biochem Sci* 32: 6–11
- King SB (2003) The nitric oxide producing reactions of hydroxyurea. *Curr Med Chem* 10: 437–452
- Kroning A, van den Boom J, Kracht M, Kueck AF, Meyer H (2022) Ubiquitin-directed AAA+ ATPase p97/VCP unfolds stable proteins crosslinked to DNA for proteolysis by SPRTN. *J Biol Chem* 298: 101976
- Kubota T, Stead DA, Hiraga S, ten Have S, Donaldson AD (2012) Quantitative proteomic analysis of yeast DNA replication proteins. *Methods* 57: 196–202
- Lafon A, Taranum S, Pietrocola F, Dingli F, Loew D, Brahma S, Bartholomew B, Papamichos-Chronakis M (2015) INO80 chromatin remodeler facilitates

- release of RNA polymerase II from chromatin for ubiquitin-mediated proteasomal degradation. *Mol Cell* 60: 784–796
- Larsen NB, Gao AO, Sparks JL, Gallina I, Wu RA, Mann M, Raschle M, Walter JC, Duxin JP (2019) Replication-coupled DNA-protein crosslink repair by SPRTN and the proteasome in xenopus egg extracts. *Mol Cell* 73: 574–588
- Lin CP, Ban Y, Lyu YL, Desai SD, Liu LF (2008) A ubiquitin-proteasome pathway for the repair of topoisomerase I-DNA covalent complexes. *J Biol Chem* 283: 21074–21083
- Liu C, Pouliot JJ, Nash HA (2002) Repair of topoisomerase I covalent complexes in the absence of the tyrosyl-DNA phosphodiesterase Tdp1. *Proc Natl Acad Sci U S A* 99: 14970–14975
- Maddi K, Sam DK, Bonn F, Prgommet S, Tulowetzke E, Akutsu M, Lopez-Mosqueda J, Dikic I (2020) Wss1 promotes replication stress tolerance by degrading histones. *Cell Rep* 30: 3117–3126
- Malik S, Bagla S, Chaurasia P, Duan Z, Bhaumik SR (2008) Elongating RNA polymerase II is disassembled through specific degradation of its largest but not other subunits in response to DNA damage *in vivo*. *J Biol Chem* 283: 6897–6905
- Maric M, Maculins T, De Piccoli G, Labib K (2014) Cdc48 and a ubiquitin ligase drive disassembly of the CMG helicase at the end of DNA replication. *Science* 346: 1253596
- Maskey RS, Flatten KS, Sieben CJ, Peterson KL, Baker DJ, Nam HJ, Kim MS, Smyrk TC, Kojima Y, Machida Y *et al* (2017) Spartan deficiency causes accumulation of topoisomerase I cleavage complexes and tumorigenesis. *Nucleic Acids Res* 45: 4564–4576
- Meerang M, Ritz D, Paliwal S, Garajova Z, Bosshard M, Mailand N, Janscak P, Hubscher U, Meyer H, Ramadan K (2011) The ubiquitin-selective segregase VCP/p97 orchestrates the response to DNA double-strand breaks. *Nat Cell Biol* 13: 1376–1382
- Mosbech A, Gibbs-Seymour I, Kagias K, Thorslund T, Beli P, Povlsen L, Nielsen SV, Smedegaard S, Sedgwick G, Lukas C *et al* (2012) DVC1 (C1orf124) is a DNA damage-targeting p97 adaptor that promotes ubiquitin-dependent responses to replication blocks. *Nat Struct Mol Biol* 19: 1084–1092
- Mouysset J, Deichsel A, Moser S, Hoegge C, Hyman AA, Gartner A, Hoppe T (2008) Cell cycle progression requires the CDC-48/UDF-1/NPL-4 complex for efficient DNA replication. *Proc Natl Acad Sci U S A* 105: 12879–12884
- Mullally JE, Chernova T, Wilkinson KD (2006) Doa1 is a Cdc48 adapter that possesses a novel ubiquitin binding domain. *Mol Cell Biol* 26: 822–830
- Mullen JR, Chen CF, Brill SJ (2010) Wss1 is a SUMO-dependent isopeptidase that interacts genetically with the Slx5-Slx8 SUMO-targeted ubiquitin ligase. *Mol Cell Biol* 30: 3737–3748
- Murai J, Huang SYN, Das BB, Renaud A, Zhang YP, Doroshov JH, Ji JP, Takeda S, Pommier Y (2012) Trapping of PARP1 and PARP2 by clinical PARP inhibitors. *Cancer Res* 72: 5588–5599
- Nakano T, Terato H, Asagoshi K, Masaoka A, Mukuta M, Ohyama Y, Suzuki T, Makino K, Ide H (2003) DNA-protein cross-link formation mediated by oxanine. A novel genotoxic mechanism of nitric oxide-induced DNA damage. *J Biol Chem* 278: 25264–25272
- Nakano T, Morishita S, Katafuchi A, Matsubara M, Horikawa Y, Terato H, Salem AM, Izumi S, Pack SP, Makino K *et al* (2007) Nucleotide excision repair and homologous recombination systems commit differentially to the repair of DNA-protein crosslinks. *Mol Cell* 28: 147–158
- Nakano T, Katafuchi A, Matsubara M, Terato H, Tsuboi T, Masuda T, Tatsumoto T, Pack SP, Makino K, Croteau DL *et al* (2009) Homologous recombination but not nucleotide excision repair plays a pivotal role in tolerance of DNA-protein cross-links in mammalian cells. *J Biol Chem* 284: 27065–27076
- Nie M, Aslanian A, Prudden J, Heideker J, Vashisht AA, Wohlschlegel JA, Yates JR 3rd, Boddy MN (2012) Dual recruitment of Cdc48 (p97)-Ufd1-Npl4 ubiquitin-selective segregase by small ubiquitin-like modifier protein (SUMO) and ubiquitin in SUMO-targeted ubiquitin ligase-mediated genome stability functions. *J Biol Chem* 287: 29610–29619
- Nielsen I, Bentsen IB, Lisby M, Hansen S, Mundbjerg K, Andersen AH, Bjergbaek L (2009) A Flp-nick system to study repair of a single protein-bound nick *in vivo*. *Nat Methods* 6: 753–757
- O'Neill BM, Hanway D, Winzeler EA, Romesberg FE (2004) Coordinated functions of WSS1, PSY2 and TOF1 in the DNA damage response. *Nucleic Acids Res* 32: 6519–6530
- Pommier Y (2006) Topoisomerase I inhibitors: camptothecins and beyond. *Nat Rev Cancer* 6: 789–802
- Pommier Y, Huang SY, Gao R, Das BB, Murai J, Marchand C (2014) Tyrosyl-DNA-phosphodiesterases (TDP1 and TDP2). *DNA Repair (Amst)* 19: 114–129
- Pommier Y, Sun Y, Huang SN, Nitiss JL (2016) Roles of eukaryotic topoisomerases in transcription, replication and genomic stability. *Nat Rev Mol Cell Biol* 17: 703–721
- Pouliot JJ, Yao KC, Robertson CA, Nash HA (1999) Yeast gene for a Tyr-DNA phosphodiesterase that repairs topoisomerase I complexes. *Science* 286: 552–555
- Pouliot JJ, Robertson CA, Nash HA (2001) Pathways for repair of topoisomerase I covalent complexes in *Saccharomyces cerevisiae*. *Genes Cells* 6: 677–687
- Quiévryn G, Zhitkovich A (2000) Loss of DNA-protein crosslinks from formaldehyde-exposed cells occurs through spontaneous hydrolysis and an active repair process linked to proteasome function. *Carcinogenesis* 21: 1573–1580
- Ramadan K, Halder S, Wiseman K, Vaz B (2017) Strategic role of the ubiquitin-dependent segregase p97 (VCP or Cdc48) in DNA replication. *Chromosoma* 126: 17–32
- Reardon JT, Sanchar A (2006) Repair of DNA-polypeptide crosslinks by human excision nuclease. *Proc Natl Acad Sci U S A* 103: 4056–4061
- Ruggiano A, Vaz B, Kilgas S, Popovic M, Rodriguez-Berriguete G, Singh AN, Higgins GS, Kiltie AE, Ramadan K (2021) The protease SPRTN and SUMOylation coordinate DNA-protein crosslink repair to prevent genome instability. *Cell Rep* 37: 110080
- Sasagawa Y, Yamanaka K, Saito-Sasagawa Y, Ogura T (2010) Caenorhabditis elegans UBX cofactors for CDC-48/p97 control spermatogenesis. *Genes Cells* 15: 1201–1215
- Schuberth C, Buchberger A (2008) UBX domain proteins: major regulators of the AAA ATPase Cdc48/p97. *Cell Mol Life Sci* 65: 2360–2371
- Schuberth C, Richly H, Rumpf S, Buchberger A (2004) Shp1 and Ubx2 are adaptors of Cdc48 involved in ubiquitin-dependent protein degradation. *EMBO Rep* 5: 818–824
- Serbyn N, Noireterre A, Bagdiul I, Plank M, Michel AH, Loewith R, Kornmann B, Stutz F (2020) The aspartic protease Ddi1 contributes to DNA-protein crosslink repair in yeast. *Mol Cell* 77: 1066–1079
- Serbyn N, Bagdiul I, Noireterre A, Michel AH, Suhandynata RT, Zhou H, Kornmann B, Stutz F (2021) SUMO orchestrates multiple alternative DNA-protein crosslink repair pathways. *Cell Rep* 37: 110034
- Shcherbik N, Haines DS (2007) Cdc48p(Npl4p/Ufd1p) binds and segregates membrane-anchored/tethered complexes via a polyubiquitin signal present on the anchors. *Mol Cell* 25: 385–397
- Sparks JL, Chistol G, Gao AO, Raschle M, Larsen NB, Mann M, Duxin JP, Walter JC (2019) The CMG helicase bypasses DNA-protein cross-links to facilitate their repair. *Cell* 176: 167–181

- Stach L, Freemont PS (2017) The AAA+ ATPase p97, a cellular multitool. *Biochem J* 474: 2953–2976
- Staker BL, Hjerrild K, Feese MD, Behnke CA, Burgin AB Jr, Stewart L (2002) The mechanism of topoisomerase I poisoning by a camptothecin analog. *Proc Natl Acad Sci U S A* 99: 15387–15392
- Stinglele J, Jentsch S (2015) DNA-protein crosslink repair. *Nat Rev Mol Cell Biol* 16: 455–460
- Stinglele J, Schwarz MS, Bloemeke N, Wolf PG, Jentsch S (2014) A DNA-dependent protease involved in DNA-protein crosslink repair. *Cell* 158: 327–338
- Stinglele J, Habermann B, Jentsch S (2015) DNA-protein crosslink repair: proteases as DNA repair enzymes. *Trends Biochem Sci* 40: 67–71
- Stinglele J, Bellelli R, Boulton SJ (2017) Mechanisms of DNA-protein crosslink repair. *Nat Rev Mol Cell Biol* 18: 563–573
- Sun Y, Saha LK, Saha S, Jo U, Pommier Y (2020a) Debulking of topoisomerase DNA-protein crosslinks (TOP-DPC) by the proteasome, non-proteasomal and non-proteolytic pathways. *DNA Repair (Amst)* 94: 102926
- Sun Y, Saha S, Wang W, Saha LK, Huang SN, Pommier Y (2020b) Excision repair of topoisomerase DNA-protein crosslinks (TOP-DPC). *DNA Repair (Amst)* 89: 102837
- Svoboda M, Konvalinka J, Trempe JF, Grantz Saskova K (2019) The yeast proteases Ddi1 and Wss1 are both involved in the DNA replication stress response. *DNA Repair (Amst)* 80: 45–51
- Torrecilla I, Oehler J, Ramadan K (2017) The role of ubiquitin-dependent segregase p97 (VCP or Cdc48) in chromatin dynamics after DNA double strand breaks. *Philos Trans R Soc Lond B Biol Sci* 372: 20160282
- Twomey EC, Ji Z, Wales TE, Bodnar NO, Ficarro SB, Marto JA, Engen JR, Rapoport TA (2019) Substrate processing by the Cdc48 ATPase complex is initiated by ubiquitin unfolding. *Science* 365: eaax1033
- Vaz B, Halder S, Ramadan K (2013) Role of p97/VCP (Cdc48) in genome stability. *Front Genet* 4: 60
- Vaz B, Popovic M, Ramadan K (2017) DNA-protein crosslink proteolysis repair. *Trends Biochem Sci* 42: 483–495
- Verma R, Oania R, Fang R, Smith GT, Deshaies RJ (2011) Cdc48/p97 mediates UV-dependent turnover of RNA pol II. *Mol Cell* 41: 82–92
- White SR, Lauring B (2007) AAA+ ATPases: achieving diversity of function with conserved machinery. *Traffic* 8: 1657–1667
- Wilson MD, Harreman M, Taschner M, Reid J, Walker J, Erdjument-Bromage H, Tempst P, Svejstrup JQ (2013) Proteasome-mediated processing of Def1, a critical step in the cellular response to transcription stress. *Cell* 154: 983–995
- Woodman PG (2003) p97, a protein coping with multiple identities. *J Cell Sci* 116: 4283–4290
- Yamada T, Okuhara K, Iwamatsu A, Seo H, Ohta K, Shibata T, Murofushi H (2000) p97 ATPase, an ATPase involved in membrane fusion, interacts with DNA unwinding factor (DUF) that functions in DNA replication. *FEBS Lett* 466: 287–291
- Yang SW, Burgin AB Jr, Huizenga BN, Robertson CA, Yao KC, Nash HA (1996) A eukaryotic enzyme that can disjoin dead-end covalent complexes between DNA and type I topoisomerases. *Proc Natl Acad Sci U S A* 93: 11534–11539
- Yarbro JW (1992) Mechanism of action of hydroxyurea. *Semin Oncol* 19: 1–10
- Ye Y (2006) Diverse functions with a common regulator: ubiquitin takes command of an AAA ATPase. *J Struct Biol* 156: 29–40
- Yip MCJ, Bodnar NO, Rapoport TA (2020) Ddi1 is a ubiquitin-dependent protease. *Proc Natl Acad Sci U S A* 117: 7776–7781
- Zecevic A, Hagan E, Reynolds M, Poage G, Johnston T, Zhitkovich A (2010) XPA impacts formation but not proteasome-sensitive repair of DNA-protein cross-links induced by chromate. *Mutagenesis* 25: 381–388
- Zhang H, Wang Q, Kajino K, Greene MI (2000) VCP, a weak ATPase involved in multiple cellular events, interacts physically with BRCA1 in the nucleus of living cells. *DNA Cell Biol* 19: 253–263
- Zhang H, Xiong Y, Chen J (2020) DNA-protein cross-link repair: what do we know now? *Cell Biosci* 10: 3



License: This is an open access article under the terms of the [Creative Commons Attribution-NonCommercial-NoDerivs](https://creativecommons.org/licenses/by-nc-nd/4.0/) License, which permits use and distribution in any medium, provided the original work is properly cited, the use is non-commercial and no modifications or adaptations are made.